AMERICAN SOCIETY FOR MICROBIOLOGY | Journal of Virology®

VACCINES AND ANTIVIRAL AGENTS

Mucosal Priming with a Recombinant Influenza A Virus-Vectored Vaccine Elicits T-Cell and Antibody Responses to HIV-1 in Mice

Jinlin Wang,[a,b,c] Tao Shu,[a,c] Weiqi Deng,[a,c] Yali Zheng,[a,c] Min Liao,[a,c] Xianmiao Ye,[a] Lujie Han,[d] Ping He,[a,c] Xuehua Zheng,[a] Ting Li,[a] Ying Feng,[a] Fengyu Hu,[b] Pingchao Li,[a] Caijun Sun,[e] Ling Chen,[a,b,c] Feng Li,[b] Liqiang Feng[a,c]

[a]State Key Laboratory of Respiratory Diseases, Guangdong Laboratory of Computational Biomedicine, Guangzhou Institutes of Biomedicine and Health, Chinese Academy of Sciences, Guangzhou, China
[b]Guangzhou Eighth People's Hospital, Guangzhou Medical University, Guangzhou, China
[c]University of Chinese Academy of Sciences, Beijing, China
[d]Guangzhou nBiomed Ltd., Guangzhou, China
[e]School of Public Health (Shenzhen), Sun Yat-sen University, Guangzhou, China

Jilin Wang and Tao Shu contributed equally to this work. Author order was determined both alphabetically and in order of increasing seniority.
Ling Chen, Feng Li, and Liqiang Feng are co-senior authors of the paper.

ABSTRACT Recombinant influenza A viral (IAV) vectors are potential to stimulate systemic and mucosal immunity, but the packaging capacity is limited and only one or a few epitopes can be carried. Here, we report the generation of a replication-competent IAV vector that carries a full-length HIV-1 *p24* gene linked to the 5′-terminal coding region of the neuraminidase segment via a protease cleavage sequence (IAV-p24). IAV-p24 was successfully rescued and stably propagated, and P24 protein was efficiently expressed in infected mammalian cells. In BALB/c mice, IAV-p24 showed attenuated pathogenicity compared to that of the parental A/PR/8/34 (H1N1) virus. An intranasal inoculation with IAV-p24 elicited moderate HIV-specific cell-mediated immune (CMI) responses in the airway and vaginal tracts and in the spleen, and an intranasal boost with a replication-incompetent adenovirus type 2 vector expressing the HIV-1 *gag* gene (Ad2-gag) greatly improved these responses. Importantly, compared to an Ad2-gag prime plus IAV-p24 boost regimen, the IAV-p24 prime plus Ad2-gag boost regimen had a greater efficacy in eliciting HIV-specific CMI responses. P24-specific $CD8^+$ T cells and antibodies were robustly provoked both systemically and in mucosal sites and showed long-term durability, revealing that IAV-p24 may be used as a mucosa-targeted priming vaccine. Our results illustrate that IAV-p24 is able to prime systemic and mucosal immunity against HIV-1 and warrants further evaluation in nonhuman primates.

IMPORTANCE An effective HIV-1 vaccine remains elusive despite nearly 40 years of research. $CD8^+$ T cells and protective antibodies may both be desirable for preventing HIV-1 infection in susceptible mucosal sites. Recombinant influenza A virus (IAV) vector has the potential to stimulate these immune responses, but the packaging capacity is extremely limited. Here, we describe a replication-competent IAV vector expressing the HIV-1 *p24* gene (IAV-p24). Unlike most other IAV vectors that carried one or several antigenic epitopes, IAV-p24 stably expressed the full-length P24 protein, which contains multiple epitopes and is highly conserved among all known HIV-1 sequences. Compared to the parental A/PR/8/34 (H1N1) virus, IAV-p24 showed an attenuated pathogenicity in BALB/c mice. When combined with an adenovirus vector expressing the HIV-1 *gag* gene, IAV-p24 was able to prime P24-specific systemic and mucosal immune responses. IAV-p24 as an alternative priming vaccine against HIV-1 warrants further evaluation in nonhuman primates.

Citation Wang J, Shu T, Deng W, Zheng Y, Liao M, Ye X, Han L, He P, Zheng X, Li T, Feng Y, Hu F, Li P, Sun C, Chen L, Li F, Feng L. 2021. Mucosal priming with a recombinant influenza A virus-vectored vaccine elicits T-cell and antibody responses to HIV-1 in mice. J Virol 95: e00059-21. https://doi.org/10.1128/JVI.00059-21.

Editor Guido Silvestri, Emory University

Address correspondence to Feng Li, gz8h_lifeng@126.com, or Liqiang Feng, feng_liqiang@gibh.ac.cn.

Received 13 January 2021
Accepted 21 March 2021
Accepted manuscript posted online 31 March 2021
Published 24 May 2021

KEYWORDS recombinant influenza A virus, vector, human immunodeficiency virus type 1, vaccine, mucosal immune response, T cell, antibody

AIDS, caused by human immunodeficiency virus type 1 (HIV-1), remains one of the most severe infectious diseases globally. More than 38 million people were living with HIV-1 at the end of 2019 (1). Mucosal exposure is the major route of HIV-1 transmission (2). Although combined antiretroviral treatment (cART) can suppress viral replication, decrease AIDS-associated deaths, and reduce the risk of transmission, it is not curative and cannot eradicate HIV-1 reservoirs (3). Lifelong medication is needed and usually leads to economic burden, drug resistance, and unwanted toxicity (3). Vaccines that can prevent HIV-1 infection and control the epidemics are still urgently needed.

Due to the high mutation rate of HIV-1 (4), an effective vaccine may ideally provoke $CD8^+$ T-cell and protective antibody responses against the conserved antigens in susceptible mucosal sites. $CD8^+$ T cells, especially those secreting multiple effector molecules, have been reported to confer viral control in nonprogressors and in a subgroup of vaccine recipients in the STEP trial and the HVTN505 trial (5–8). In nonhuman primates (NHPs) challenged with simian immunodeficiency virus (SIV), $CD8^+$ T cells are associated with the protective efficacy of several experimental vaccines (9–11). On the other hand, protective antibodies against the conserved and vulnerable epitopes on the envelope (Env) can block HIV-1 entry into host cells or trigger antibody-dependent cell-mediated cytotoxicity of infected cells (12–14). To stimulate such immune responses, recombinant viral vectors, including replication-incompetent human adenoviruses (Ad), have been explored (15). However, the quantity and quality of $CD8^+$ T cells elicited by a replication-incompetent viral vector may be limited and may be dampened by preexisting anti-vector neutralizing antibodies (11, 16). These issues may be resolved by exploring prime-boost vaccine regimens using two or more different viral vectors, especially replication-competent ones with minimal preexisting immunity in humans (17, 18). A heterologous prime-boost regimen consisting of a replication-competent modified vaccinia virus Tian Tan (MVTT) vector and an Ad5 vector achieved 50% protection in SIV-infected NHPs (9). Thus, replication-competent viral vectors that can circumvent the preexisting immunity may be suitable as a vector for HIV-1 vaccine.

Recently, with progress in reverse genetics technology for influenza A virus (IAV) (19), recombinant IAV has been explored as a vaccine vector against a variety of pathogens, including HIV-1 (20–26). IAV belongs to the *Orthomyxoviridae* family, of which the genome contains 8 single-stranded negative-sense viral RNA (vRNA) segments. The 4th and 6th segments encode the major surface glycoproteins, hemagglutinin (HA) and neuraminidase (NA), respectively. HA mediates IAV binding and entry and is targeted by neutralizing antibodies. NA facilitates progeny virion release by destroying sialic acids, the receptors recognized by HA. NA is targeted by nonneutralizing but protective antibodies (27). HA and NA of one IAV can be replaced with those from an antigenically distinct IAV, and thus, the preexisting neutralizing antibodies can be easily bypassed (28). There is no DNA phase in the life cycle of IAV; therefore, there is no risk of viral integration into the host genome (28). IAV vRNAs can trigger the production of type I interferon (IFN) and help to induce a high level of immune responses (28). Several IAV vectors carrying epitopes of HIV-1 or SIV have been shown to elicit systemic and mucosal immune responses (22–25). However, their exogenous insert capacity is limited. Most IAV vectors carry only one or a few epitopes (22–24). Immunization with IAV vectors carrying three cytotoxic T lymphocyte (CTL) epitopes is insufficient to protect against SIV infection, possibly because the CTL response is not broad enough (24). An improved strategy might rely on the incorporation of multiple conserved epitopes or even a full-length HIV-1 antigen.

We previously developed a replication-competent IAV vector based on A/PR/8/34 (H1N1) virus (PR8), which can carry a foreign sequence up to ~800 nucleotides (nt) in length, such as the coding sequence for enhanced green fluorescent protein (EGFP; 723 nt) or *Gaussia* luciferase (564 nt) (29, 30). This IAV vector grows to a high titer in

embryonic eggs and expresses the reporter genes in the lungs of infected mice (30). In this study, we used this vector to carry the coding sequence for HIV-1 P24 capsid protein (IAV-p24), a major core protein released from the Gag polyprotein by protease-mediated cleavage. The *p24* gene is highly conserved among different variants, and the length (678 nt) does not exceed the packaging capacity of our IAV vector (31). We examined the growth property of IAV-p24 in cell cultures and embryonic eggs and assessed its immunogenicity in BALB/c mice. We also explored a heterologous prime-boost regimen using IAV-p24 and a replication-incompetent Ad2 vector expressing the HIV-1 *gag* gene (Ad2-gag) and tested the capability in inducing P24-specific systemic and mucosal immune responses.

RESULTS

Generation of IAV-p24. We used the NA segment to carry a full-length HIV-1 *p24* gene that contains multiple conserved CTL epitopes (31). The *p24* gene was optimized and linked to the 5′-terminal coding region of NA vRNA (Fig. 1A). The noncoding regions (NCR) and 157 nt of the 5′-terminal coding region were maintained for efficient packaging of the chimeric NA vRNA (Fig. 1A). A "self-cleavage" protease P2A sequence was inserted between the *NA* and *p24* genes to generate individual NA and P24 proteins after translation (Fig. 1A). IAV-p24 was rescued by cotransfecting the chimeric NA plasmid and plasmids encoding the other seven vRNAs into a coculture of human embryonic kidney (HEK293) and Madin-Darby canine kidney (MDCK) cells. In MDCK cells, IAV-p24 formed slightly smaller plaques than wild-type PR8 did (Fig. 1B). IAV-p24 infection led to efficient expression of the P24 protein (Fig. 1C). Two bands were detected by a P24-specific monoclonal antibody. The ~25-kDa band represents the P24 protein, which has a molecular weight of 24 kDa, whereas the ~85-kDa band possibly represents the NA-P24 fusion protein that results from the incomplete cleavage by 2A peptide. Most or all MDCK cells infected with IAV-p24 expressed both HA and P24 proteins (Fig. 1D). In embryonic eggs, the *p24* gene appeared to be stably maintained in the chimeric NA vRNA for 9 passages (Fig. 1E). No mutations were observed in either the NA- or P24-encoding sequence (data not shown). Notably, IAV-p24 showed a lower growth capacity than PR8 did (Fig. 1F). The peak yield of IAV-p24 reached 1×10^7 PFU per ml of allantoic fluid, which was ~1 log lower than that of PR8 (Fig. 1F). Thus, IAV-p24 stably carries the *p24* gene and is attenuated in cell cultures and embryonic eggs.

The pathogenicity of IAV-p24 is attenuated in BALB/c mice. To test if the insertion of HIV-1 *p24* gene affects the virulence of IAV-p24, 8-week-old female BALB/c mice were intranasally (i.n.) infected with IAV-p24 at 10-fold-increasing doses from 1×10^3 to 1×10^5 PFU per mouse or with PR8 at 1×10^3 PFU per mouse. All mice infected with PR8 experienced a severe loss of body weight and gradually died before day 6 after infection (Fig. 2A and B). In contrast, none of the mice infected with the same dose of IAV-p24 died or showed any symptoms throughout the experiment. Mice infected with 1×10^4 PFU of IAV-p24 showed a transient loss of body weight and gradually recovered. Four of five mice that received 1×10^5 PFU of IAV-p24 died (Fig. 2A and B). Consistently, on day 5 after infection, much fewer live viral particles were detected in mice infected with IAV-p24 than in those infected with PR8 (Fig. 2C). Together, these findings show that compared to wild-type PR8, IAV-p24 has a significantly attenuated phenotype in mice.

A single i.n. immunization with IAV-p24 induces moderate but significant HIV-specific CMI responses. To test the immunogenicity of IAV-p24, 8-week-old female BALB/c mice were i.n. inoculated with1×10^4 PFU of IAV-p24. We used this dose to enable sufficient expression of P24 protein without causing severe diseases (Fig. 2). Two weeks later, lymphocytes were isolated from the bronchoalveolar lavage fluid (BALF), mediastinal lymph nodes (MLN), and the spleen and were assessed by an IFN-γ enzyme-linked immunosorbent spot (ELISpot) assay and major histocompatibility complex (MHC)-tetramer staining. Because the number of lymphocytes in the BALF was limited, they were analyzed only by MHC-tetramer staining. Upon stimulation with HIV-1 Gag peptide pools, significant IFN-γ-secreting cells were detected in the MLN

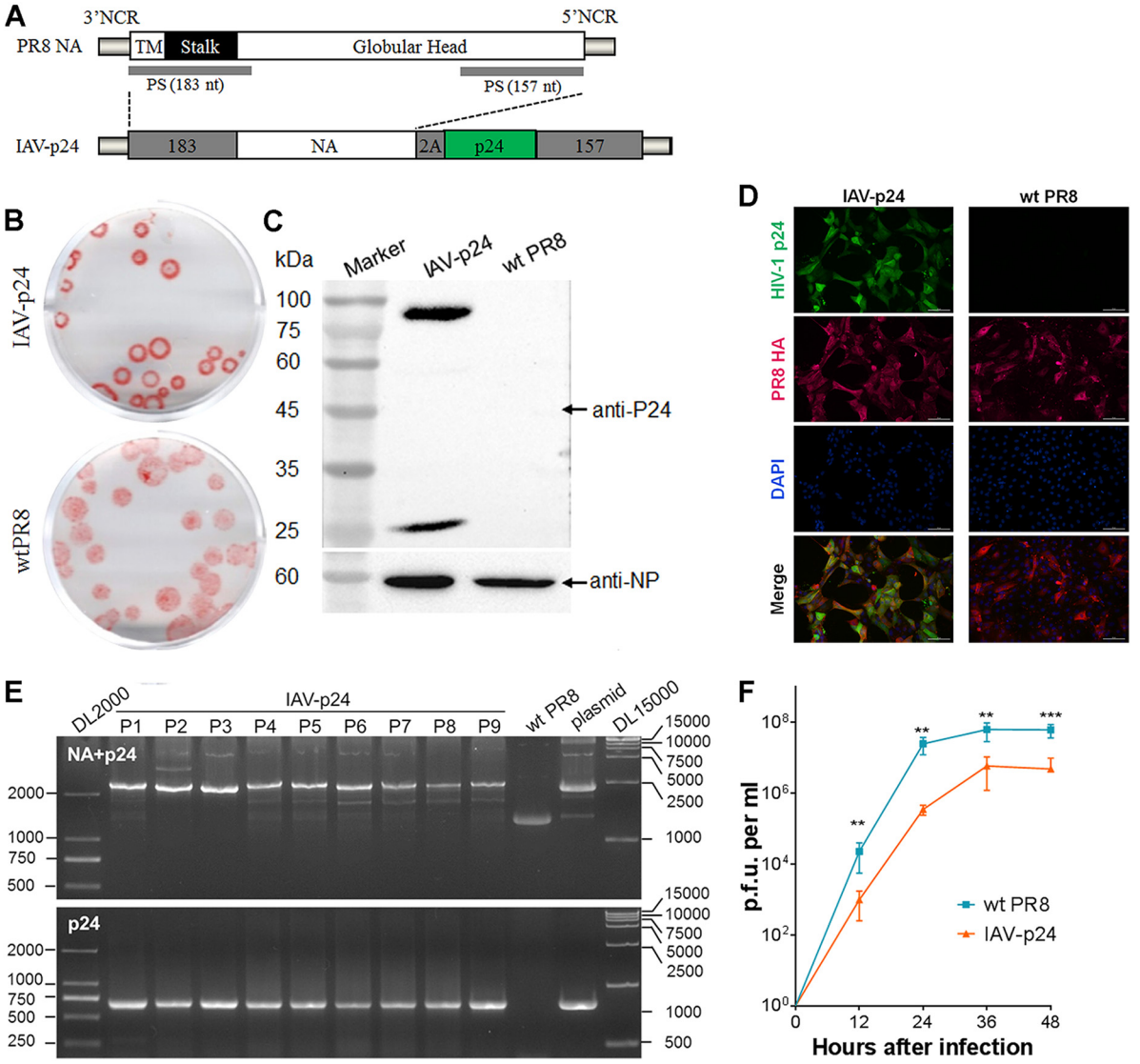

FIG 1 Generation and characterization of IAV-p24. (A) Schematic diagram of the native and chimeric NA vRNA. Each element is shown. TM, transmembrane motif; PS, packaging signal. (B) Plaques formed by IAV-p24 (top) and wild-type (wt) PR8 (bottom) in MDCK cells. At 72 h after infection, the plaques were labeled with anti-PR8 mouse serum and developed using an AEC kit. (C) Expression of the P24 protein in MDCK cells infected with IAV-p24. Cells were infected with IAV-p24 or PR8 at 0.5 PFU per cell. At 24 h after infection, P24 protein was examined by Western blot analysis. The IAV nucleoprotein (NP) was examined in parallel. (D) Immunofluorescence images of MDCK cells infected with IAV-p24 or PR8. Cells were infected with IAV-p24 or PR8 at 0.1 PFU per cell. At 36 h after infection, P24 and HA proteins were examined using a mouse anti-P24 monoclonal antibody and a rabbit anti-HA polyclonal antibody, respectively. (E) Genome stability analysis. IAV-p24 was serially passaged in embryonic eggs 9 times. Total RNA was extracted from the allantoic fluids. Chimeric NA-p24 fragment (top) and the *p24* gene (bottom) were amplified by RT-PCR and examined. The genomic plasmid pM-PR8NA+p24 and PR8 virus were examined in parallel as controls. (F) Growth curves of IAV-p24 and PR8 in embryonic eggs. Nine-day-old embryonic eggs were infected with IAV-p24 or PR8 at 50 PFU per egg. Live viral particles in the allantoic fluids were titrated by plaque-forming assay. Data are representative of those from two independent experiments and expressed as the means ± standard deviation (SD) ($n = 5$). Comparison between groups was conducted using unpaired two-tailed Student's *t* test. **, $P < 0.01$; ***, $P < 0.001$.

and spleen (Fig. 3A and B), suggesting that one dose of IAV-p24 elicits pulmonary and systemic cell-mediated immune (CMI) responses against P24. Notably, significant P24-specific $CD8^+$ T cells (3.87% of total $CD8^+$ T cells) were detected in the BALF (Fig. 3C). Only residual P24-specific $CD8^+$ T cells were detected in the MLN. These cells were also detected in the spleen (0.61% of total $CD8^+$ T cells), but the frequency was much lower than that in the BALF (Fig. 3C), revealing that an i.n. immunization with IAV-p24 tends to elicit a $CD8^+$ T-cell response in the airway tracts. Thus, a single i.n. immunization

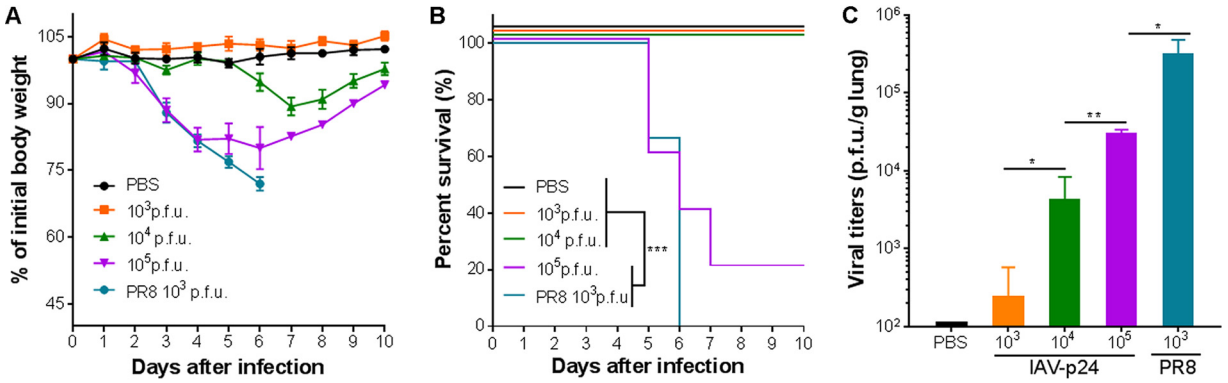

FIG 2 Pathogenicity of IAV-p24 in BALB/c mice. (A) Body weight of the mice infected with IAV-p24 or PR8. Eight-week-old female BALB/c mice were used and the body weight was monitored daily. (B) Survival curves of the mice infected with IAV-p24 or PR8. Mice that lost 25% of initial body weight or showed severe symptoms were scored as dead and euthanized. (C) Viral loads in the lung. At 5 days after infection, mice were sacrificed and the lung tissues were separated and homogenized. Live viral particles were assessed by plaque-forming assay. Data are representative of those from two independent experiments and expressed as the means ± SD ($n = 5$). Comparisons among groups in panels B and C were conducted using the log rank test and one-way analysis of variance (ANOVA), respectively. *, $P < 0.05$; **, $P < 0.01$; ***, $P < 0.001$.

with IAV-p24 induces an HIV-specific CD8$^+$ T-cell response in the airway mucosa and, to a lesser degree, in the spleen.

An i.n. prime with IAV-p24 followed by an i.n. boost with Ad2-gag induces robust HIV-specific CMI responses. Because a prime-boost regimen with two heterologous viral vectors has the potential to elicit much stronger immune responses than each single viral vector (9), we speculated that IAV-p24, when combined with another virus-vectored vaccine, may elicit an enhanced immune response. To determine if IAV-p24 is suitable as a priming vaccine or a booster vaccine, we used Ad2-gag as part of two prime-boost regimens with IAV-p24. Eight-week-old female BALB/c mice were i.n. primed with IAV-p24 at 1×10^4 PFU per mouse or with Ad2-gag at 1×10^7 viral particles (v.p.) per mouse. Three weeks later, the mice were i.n. boosted with the same dose of Ad2-gag or IAV-p24 (Fig. 4A). We used this dosage because at these doses each single vector elicited only moderate CMI responses against P24 (Fig. 3 and data not shown), and thus, the effects of a booster immunization can be easily monitored. Mice that received phosphate-buffered saline (PBS) followed by one dose of either IAV-p24 or Ad2-gag were used as single-immunization controls, whereas those that received two doses of PR8 (50 PFU per mouse) or Ad2-empty (1×10^7 v.p. per mouse) were used as mock-immunization controls (Fig. 4A). Two weeks after the final immunization, much more IFN-γ-secreting cells were detected in the MLN and spleens of the two prime-boost groups than in those of the two single-immunization groups (Fig. 4B and C), suggesting that the prime-boost regimens elicit higher levels of CMI responses than each single vector. Interestingly, significantly more IFN-γ-secreting cells were observed in mice that received the IAV-p24 prime plus Ad2-gag boost regimen than in mice that received the Ad2-gag prime plus IAV-p24 boost regimen (Fig. 4B and C), implying that IAV-p24 may be preferably used as a priming vaccine for Ad2-gag.

We next assessed the P24-specific CD8$^+$ T-cell response. The IAV-p24 prime plus Ad2-gag boost regimen induced the most robust P24-specific CD8$^+$ T-cell response in the BALF, MLN, and spleen (Fig. 4D and E). The Ad2-gag prime plus IAV-p24 boost regimen also induced this response, but the level was lower than with the IAV-p24 prime plus Ad2-gag boost regimen (Fig. 4D and E). Consistent with the results in Fig. 3, one dose of IAV-p24 induced a detectable P24-specific CD8$^+$ T-cell response in the BALF and spleen but not in the MLN, whereas one dose of Ad2-gag only induced a detectable P24-specific CD8$^+$ T-cell response in the BALF (Fig. 4D and E). Notably, in mice that received the prime-boost regimens, the frequency of P24-specific CD8$^+$ T cells in the BALF was much higher than that in the MLN and spleen (Fig. 4D and E), implying that

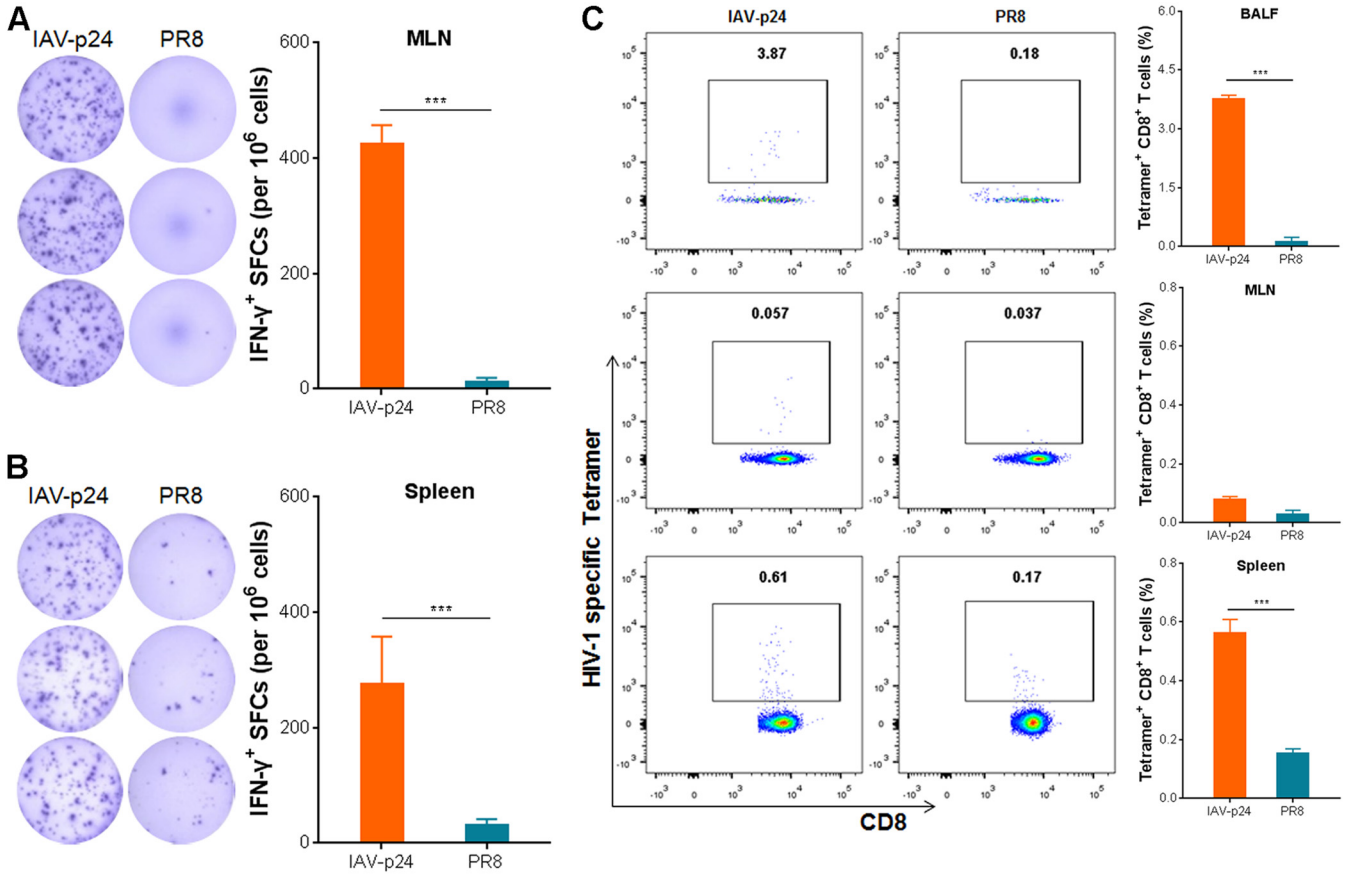

FIG 3 Immunogenicity of IAV-p24 in BALB/c mice. (A) IFN-γ-secreting cells in the MLN. (B) IFN-γ-secreting cells in the spleen. Eight-week-old BALB/c mice were i.n. immunized with 1×10^4 PFU of IAV-p24 or 50 PFU of PR8. Two weeks later, mice were sacrificed. Lymphocytes were isolated and examined by ELISpot assay using HIV-1 Gag-derived peptide pools. Representative wells (left) and the frequencies of IFN-γ^+ spot-forming cells (SFCs; right) are shown. (C) P24-specific CD8$^+$ T cells in total CD8$^+$ T cells from the BALF (top), MLN (middle), and spleen (bottom). Lymphocytes were labeled with an MHC-I H-2K^d tetramer containing a gag peptide (amino acid sequence: AMQMLKETI) and analyzed by flow cytometry. Representative flow cytometry dot plot graphs (left) and the frequencies of tetramer$^+$ CD8$^+$ T cells (right) are shown. Data are representative of those from three independent experiments and expressed as the means $\pm$ SD ($n = 5$). Comparisons between groups were conducted using unpaired two-tailed Student's t test. ***, $P < 0.001$.

both prime-boost regimens tend to induce HIV-specific CD8$^+$ T-cell response in the airway mucosa.

To test if the HIV-specific CD8$^+$ T cells are able to produce cytokines, we performed an intracellular cytokine staining (ICS) assay. Because only the mice that received IAV-p24 or PR8 had enough lymphocytes in the BALF and MLN, four groups were included: the IAV-p24 prime plus Ad2-gag boost group, the Ad2-gag prime plus IAV-p24 boost group, the IAV-p24 alone group, and the control PR8 group. Upon stimulation with HIV-1 Gag peptide pools, much more IFN-γ-secreting CD8$^+$ T cells were detected in the BALF of the prime-boost groups than in that of the IAV-p24 alone group (Fig. 5A). Notably, much more CD8$^+$ T cells secreting both IFN-γ and tumor necrosis factor alpha (TNF-α) were observed in the prime-boost groups (8.2% and 5.3% in the IAV-p24 prime plus Ad2-gag boost group and the Ad2-gag prime plus IAV-p24 boost group, respectively) than in the IAV-p24 alone group (0.4%) (Fig. 5A). Despite the low frequency, a subset of CD8$^+$ T cells in the prime-boost groups simultaneously secreted IFN-γ, TNF-α, and interleukin 2 (IL-2) (Fig. 5A), suggesting that the prime-boost regimens elicit a CD8$^+$ T-cell response with a relatively high quality. IFN-γ-secreting CD8$^+$ T cells were also detected in the MLN and spleens of the prime-boost groups, whereas only a small number of these cells were observed in the spleens but not in the MLN of the IAV-p24 alone group (Fig. 5B and C). Thus, the prime-boost regimens are able to induce cytokine-secreting CD8$^+$ T cells in the airway mucosa.

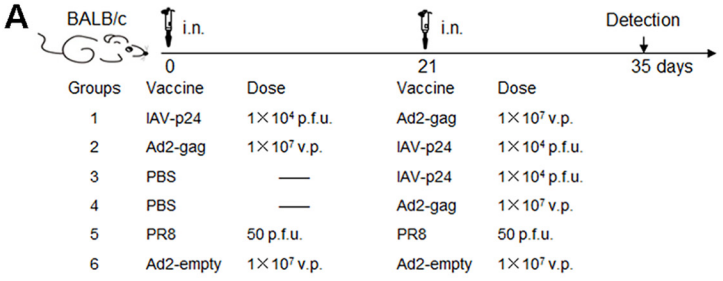

Groups	Vaccine	Dose	Vaccine	Dose
1	IAV-p24	1×10^4 p.f.u.	Ad2-gag	1×10^7 v.p.
2	Ad2-gag	1×10^7 v.p.	IAV-p24	1×10^4 p.f.u.
3	PBS	——	IAV-p24	1×10^4 p.f.u.
4	PBS	——	Ad2-gag	1×10^7 v.p.
5	PR8	50 p.f.u.	PR8	50 p.f.u.
6	Ad2-empty	1×10^7 v.p.	Ad2-empty	1×10^7 v.p.

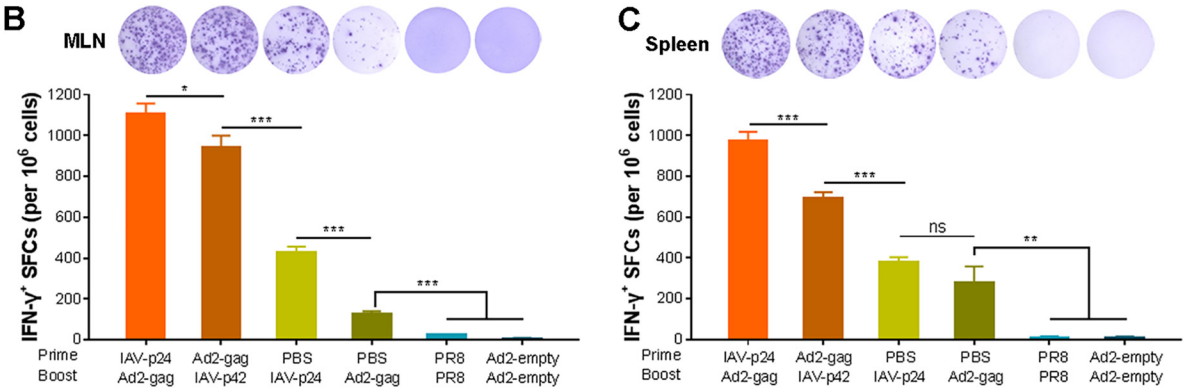

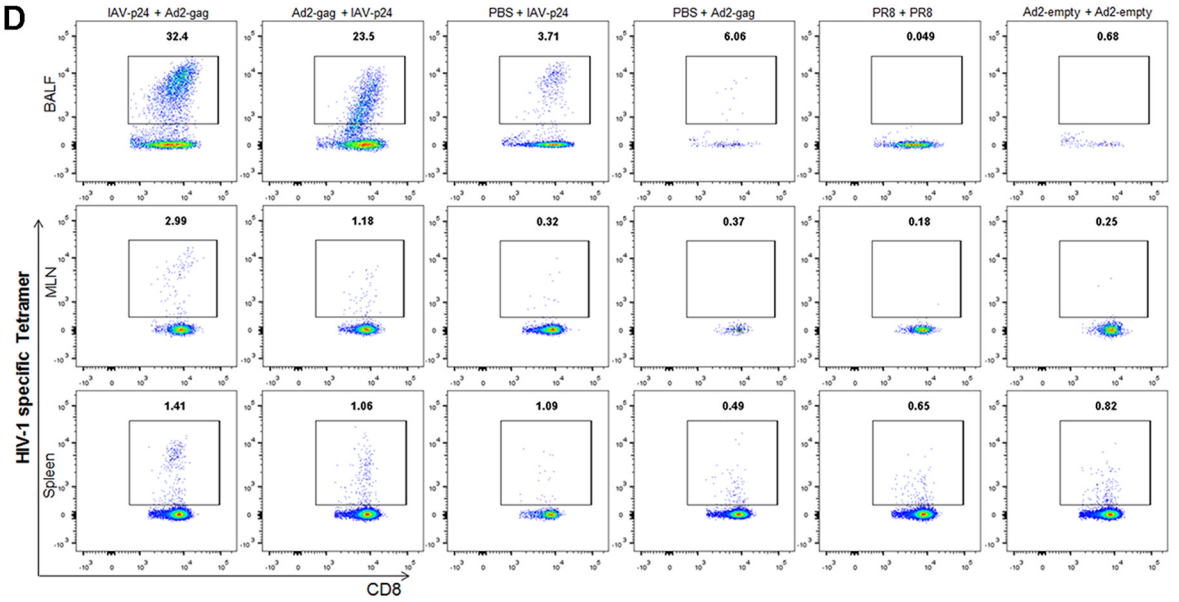

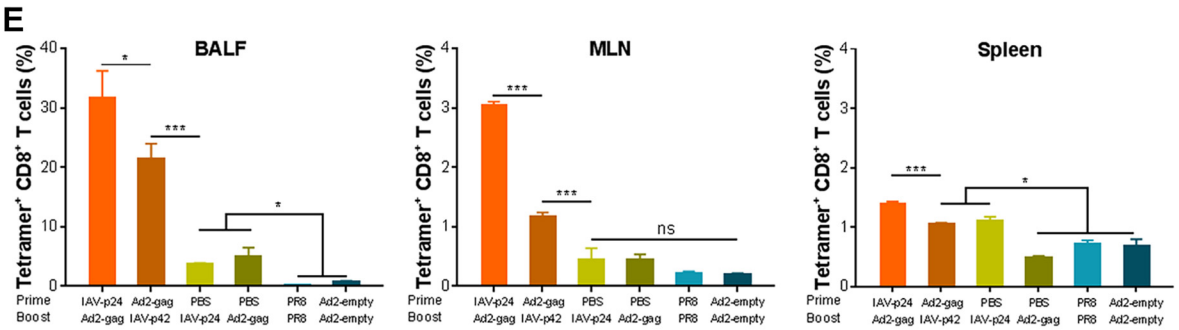

FIG 4 CMI responses elicited by the heterologous prime-boost regimens consisting of IAV-p24 and Ad2-gag in mice. (A) Schematic diagram of the heterologous prime-boost regimens. The dose of each vaccine and the schedules for immunization and detection are

(Continued on next page)

The IAV-p24 prime plus Ad2-gag boost regimen elicits P24-specific IgA and IgG responses. We then tested the antibody responses against HIV-1 P24 in the BALF and serum samples by an enzyme-linked immunosorbent assay (ELISA). P24-specific IgA antibodies were detected in the BALF of all the mice that received the IAV-p24 prime plus Ad2-gag boost regimen and 3 of 5 mice that received the Ad2-gag prime plus IAV-p24 boost regimen but not in that of the single-immunization mice or control mice (Fig. 6A), suggesting that both prime-boost regimens elicit an HIV-specific IgA response, but the IAV-p24 prime plus Ad2-gag boost regimen appears to have a greater potency. Comparable P24-specific IgG antibodies were observed in the sera of the two prime-boost groups but not in those of the single-immunization groups (Fig. 6B). Thus, the prime-boost regimens elicit detectable P24-specific antibody responses. One dose of IAV-p24, however, is unable to elicit these responses, or these responses were not detectable yet in this group at 2 weeks after immunization.

The mucosal and systemic immunity elicited by the IAV-p24 prime plus Ad2-gag boost regimen is durable. To explore the dynamics of the immunization-elicited HIV-specific immunity, 8-week-old female BALB/c mice were immunized with the IAV-p24 prime plus Ad2-gag boost regimen or with IAV-p24 alone (Fig. 7A). Mice that received PR8 and Ad2-empty were used as controls. At 1, 3, and 11 weeks after the final immunization, the CMI responses in the BALF, MLN, and spleen were assessed. IFN-γ-secreting cells could be detected in the BALF of both immunization groups as early as 1 week after immunization and sharply increased at 3 weeks (Fig. 7B). These cells were also detected in the MLN and seemed to peak at 1 week after immunization and decreased thereafter (Fig. 7C). The IFN-γ-secreting cells in the BALF and MLN at 11 weeks after immunization were hard to determine due to the lack of enough lymphocytes. In the spleens of the prime-boost group, IFN-γ-secreting cells remained a high level at each time point, whereas in those of the IAV-p24 alone group, these cells were detectable at 1 and 3 weeks after immunization but disappeared at 11 weeks (Fig. 7D). Notably, at each time point, many more IFN-γ-secreting cells were observed in the prime-boost group than in the IAV-p24 alone group (Fig. 7B to D). Thus, the HIV-specific CMI responses elicited by the prime-boost regimen, at least in the spleen, maintain a high level for a long period.

We next tested the duration of the P24-specific $CD8^+$ T-cell response. In the BALF of the prime-boost group, P24-specific $CD8^+$ T cells became detectable at 1 week after immunization, peaked at 3 weeks and remained high even at 11 weeks (Fig. 7E), revealing a long-lasting $CD8^+$ T-cell response in the airway tracts. In the BALF of the IAV-p24 alone group, these cells were not detected until 3 weeks after immunization and remained detectable at 11 weeks, but the frequency was lower than that in the prime-boost group (Fig. 7E). In the MLN of the prime-boost group, these cells were detected at 3 weeks after immunization, whereas in those of the IAV-p24 alone group, they were barely detectable at any time point (Fig. 7F). In the spleens of the prime-boost group, these cells were detected throughout the experiment, whereas in those of the IAV-p24 alone group they were detectable only at 3 weeks after immunization (Fig. 7G). Together, these results show that the prime-boost regimen elicits a robust and long-lasting P24-specific $CD8^+$ T-cell response. IAV-p24 alone also elicits this response, but the level and durability are not as good as with the prime-boost regimen.

To test if the P24-specific $CD8^+$ T-cell response is also elicited in the genital tract, the most susceptible site for HIV-1 infection, lymphocytes from the vaginal tissues were assessed. Significant P24-specific $CD8^+$ T cells were detected in the prime-boost

FIG 4 Legend (Continued)

shown. (B) IFN-γ-secreting cells in the MLN. (C) IFN-γ-secreting cells in the spleen. At 2 weeks after the booster immunization, mice were sacrificed. Lymphocytes were isolated and examined by ELISpot assay. Representative wells (top) and the frequencies of IFN-γ^+ SFCs (bottom) are shown. (D) Representative flow cytometry dot plot graphs of tetramer$^+$ $CD8^+$ T cells in the BALF (top), MLN (middle), and spleen (bottom). (E) Frequencies of tetramer$^+$ $CD8^+$ T cells in the BALF (left), MLN (middle), and spleen (right). P24-specific $CD8^+$ T cells were assessed by MHC-tetramer staining. Data are representative of those from three independent experiments and expressed as the means $\pm$ SD ($n = 5$). Comparisons among groups were conducted using one-way ANOVA. *, $P < 0.05$; **, $P < 0.01$; ***, $P < 0.001$. ns, no significance.

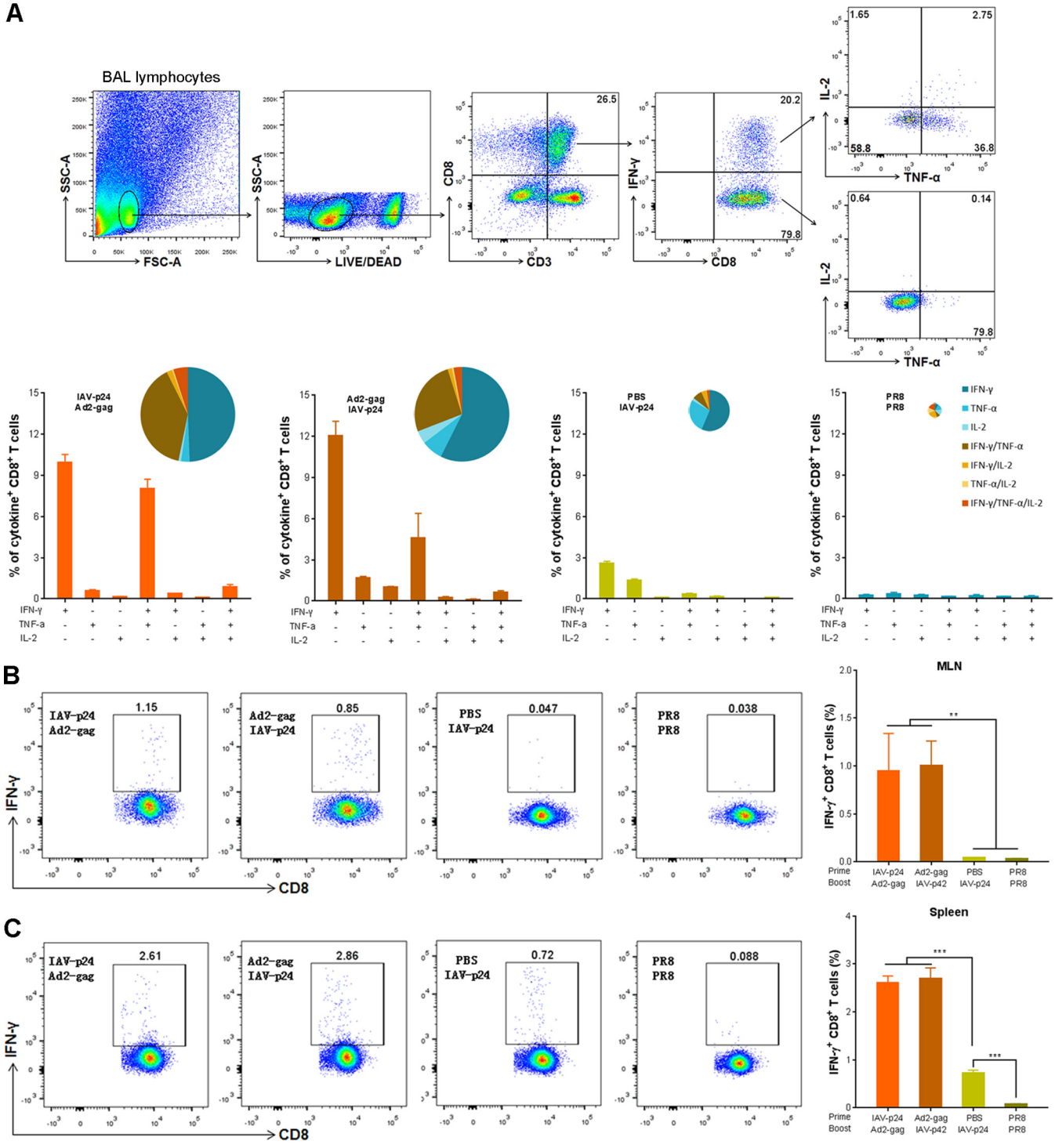

FIG 5 Cytokine secretion profiles of HIV-specific $CD8^+$ T cells. (A) Cytokine-secreting $CD8^+$ T cells in the BALF. BALF lymphocytes were stimulated with HIV-1 Gag peptide pools. At 10 h after stimulation, cells were labeled with surface antibodies and cytokine-specific monoclonal antibodies and analyzed by flow cytometry. The gating strategy (top) and the frequencies of $CD8^+$ T cells secreting one, two, or three cytokines (bottom) are shown. The pie charts indicate the percentages of $CD8^+$ T cells secreting one, two, or three cytokines among the total cytokine-secreting $CD8^+$ T cells. (B) IFN-γ-secreting $CD8^+$ T cells in the MLN. (C) IFN-γ-secreting $CD8^+$ T cells in the spleen. Representative flow cytometry dot plot graphs (left) and the frequencies of IFN-γ^+ $CD8^+$ T cells (right) are shown. Data are representative of those from three independent experiments and expressed as the means ± SD ($n = 5$). Comparisons among groups were conducted using one-way ANOVA. **, $P < 0.01$; ***, $P < 0.001$.

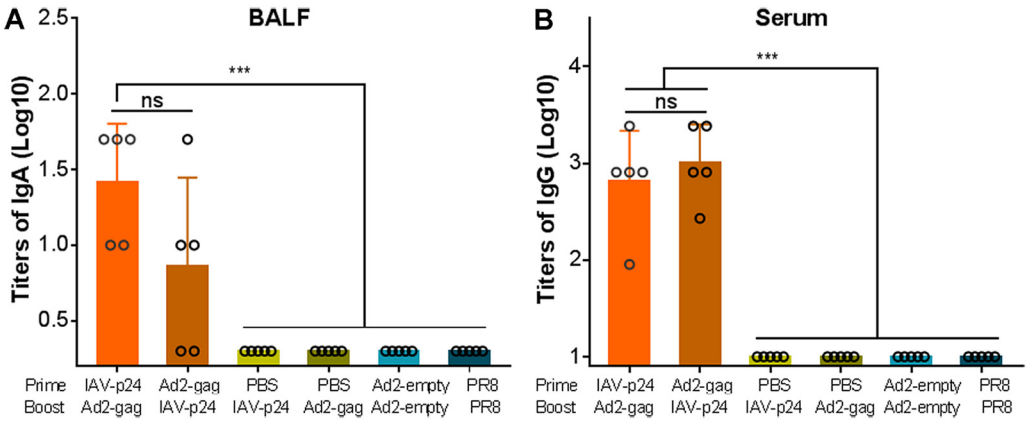

FIG 6 P24-specific antibody responses elicited by the heterologous prime-boost regimens. (A) P24-specific IgA antibodies in the BALF. (B) P24-specific IgG antibodies in the serum. BALF and serum samples were serially diluted, and the P24-specific IgA and IgG antibodies were assessed by ELISA using horseradish peroxidase (HRP)-conjugated goat anti-mouse IgA and IgG antibodies, respectively. The endpoint titers were calculated as the reciprocal of the highest dilution at which the optical density values at 450 nm (OD_{450}) were equal to or higher than three times those of the control wells. Each circle represents the mean value of three technical replicates from an individual mice. Data are representative of those from three independent experiments and expressed as means ± SD ($n = 5$). Comparisons among groups were conducted using one-way ANOVA. ***, $P < 0.001$.

group at each time point, although the frequency showed a bit of a decrease at 11 weeks after immunization (Fig. 7H). However, these cells were detected in the IAV-p24 alone group only at 3 weeks after immunization and decreased to be barely detectable at 11 weeks (Fig. 7H). Thus, both the prime-boost regimen and IAV-p24 alone can elicit a P24-specific $CD8^+$ T-cell response in the vaginal mucosa, but the prime-boost regimen provokes this response more robustly and with a better durability.

We also examined the dynamics of the P24-specific antibody responses. In the BALF of the prime-boost group, P24-specific IgA antibodies were detected for half of the mice at 1 week after immunization and for all the mice at 3 weeks and remained detectable for half of the mice even at 11 weeks (Fig. 8A). In the BALF of the IAV-p24 alone group, these antibodies were detected for only 1 of 8 mice at 1 weeks and for 6 of 8 mice at 3 weeks but turned to be undetectable at 11 weeks (Fig. 8A). This result suggests that the prime-boost regimen elicits the P24-specific IgA response with a better durability than IAV-p24 alone does. In the sera of the prime-boost group, P24-specific IgG antibodies became detectable for 6 of 8 mice as early as 1 week after immunization, sharply increased at 3 weeks, and remained a high level even at 11 weeks (Fig. 8B). In the serum of the IAV-p24 alone group, these antibodies were not detected at 1 week but became detectable for half of the mice at 3 weeks and kept increasing at 11 weeks, although the titers were lower than those in the prime-boost group (Fig. 8B). Thus, the prime-boost regimen provokes the P24-specific IgG response more rapidly and robustly than IAV-p24 alone does. These results, in addition to the results shown in Fig. 6, support the notion that a single dose of IAV-p24 elicits mild and delayed P24-specific antibody responses. Significant P24-specific IgA antibodies were detected in the vaginal lavage fluid (VALF) of both immunization groups at 1 and 3 weeks after immunization but not at 11 weeks (Fig. 8C), although a comparison is not available due to the lack of enough VALF samples. This result suggests that the prime-boost regimen and IAV-p24 alone, although administered via an i.n. route, can elicit a P24-specific IgA response in the vaginal tract.

The immunogenicity of IAV-p24 is not impacted by the preexisting antibodies against an H3N2 strain. To test the effects of the preexisting antibody response against a homologous or heterologous IAV on the immunogenicity of IAV-p24, 6-week-old female BALB/c mice were intramuscularly (i.m.) preimmunized with inactivated PR8 or H3N2 (strain A/Hong Kong/4801/2014) virus or PBS at 9 weeks before they received 1×10^3 or 1×10^4 PFU of IAV-p24 (Fig. 9A). At 1 week before IAV-p24 immunization, H1 HA-specific antibodies were detected in mice preimmunized with PR8

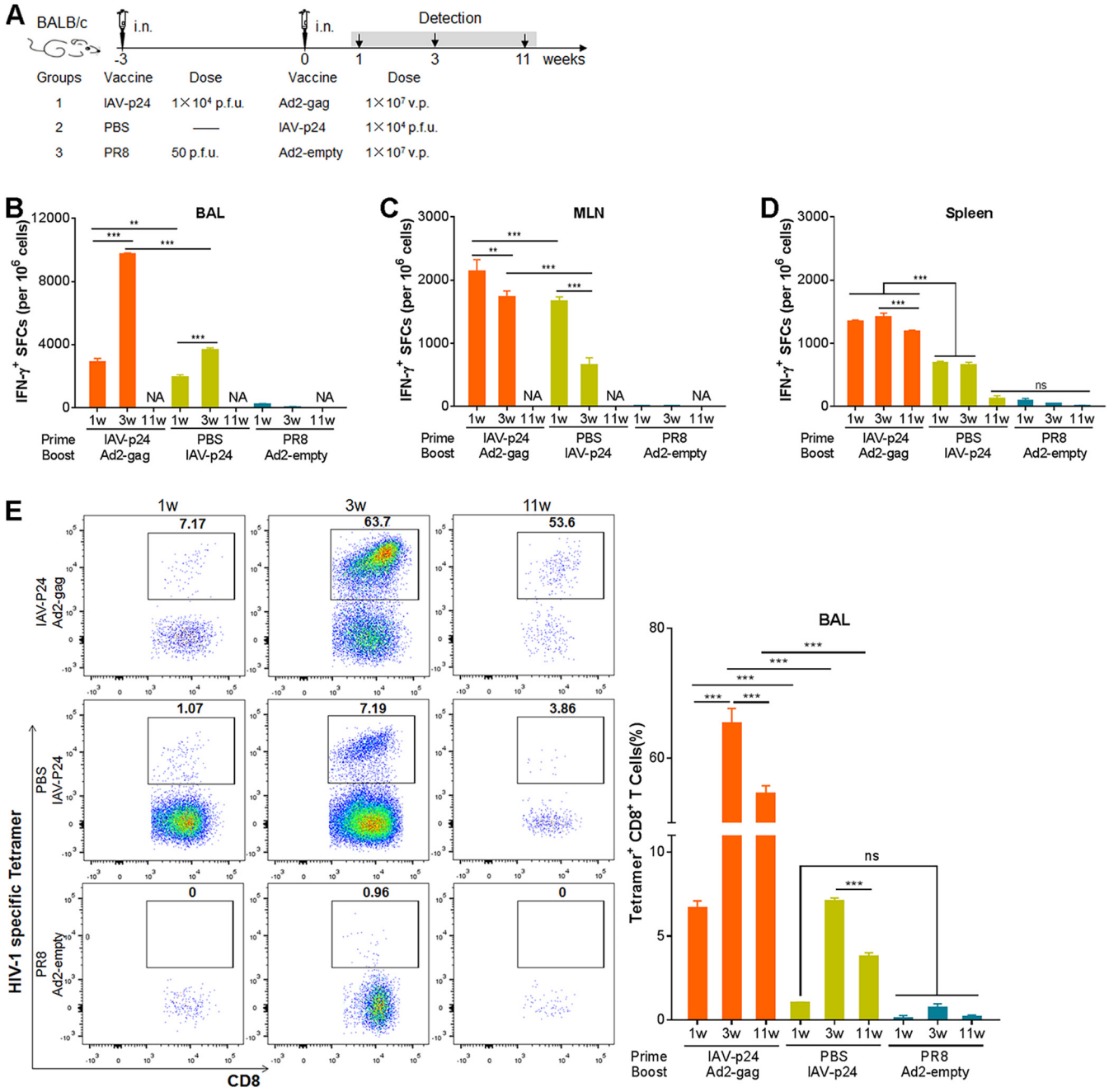

FIG 7 Dynamics of the CMI responses elicited by the IAV-p24 prime plus Ad2-gag boost regimen. (A) Schematic diagram of the immunization and detection. At 1, 3, and 11 weeks after the booster immunization, mice were sacrificed and lymphocytes were isolated. (B) IFN-γ-secreting cells in the BALF. (C) IFN-γ-secreting cells in the MLN. (D) IFN-γ-secreting cells in the spleen. Lymphocytes were examined by ELISpot assay. NA, not analyzed. (E) P24-specific $CD8^+$ T cells in total $CD8^+$ T cells from the BALF. (F) P24-specific $CD8^+$ T cells in total $CD8^+$ T cells from the MLN. (G) P24-specific $CD8^+$ T cells in total $CD8^+$ T cells from the spleen. (H) P24-specific $CD8^+$ T cells in total $CD8^+$ T cells from the vaginal tract. P24-specific $CD8^+$ T cells were assessed by MHC-tetramer staining. In each panel, representative flow cytometry dot plot graphs (left) and the frequencies of tetramer$^+$ $CD8^+$ T cells (right) are shown. Data are representative of those from two independent experiments and expressed as means ± SD ($n = 8$). Comparisons among groups were conducted using one-way ANOVA. **, $P < 0.01$; ***, $P < 0.001$.

but not in those with H3N2, whereas H3 HA-specific antibodies were detected in mice preimmunized with H3N2 but not in those with PR8 (Fig. 9B). Only residual HIV-specific IFN-γ-secreting cells were induced in the MLN and spleens of mice preimmunized with PR8 (Fig. 9C and D), revealing the deleterious effects of the preexisting anti-vector antibodies. However, these cells were dose dependently elicited regardless of the immune status against H3N2 (Fig. 9C and D), suggesting that IAV-p24 has comparable immunogenicities in the presence and absence of H3N2-specific antibodies. We next tested the P24-

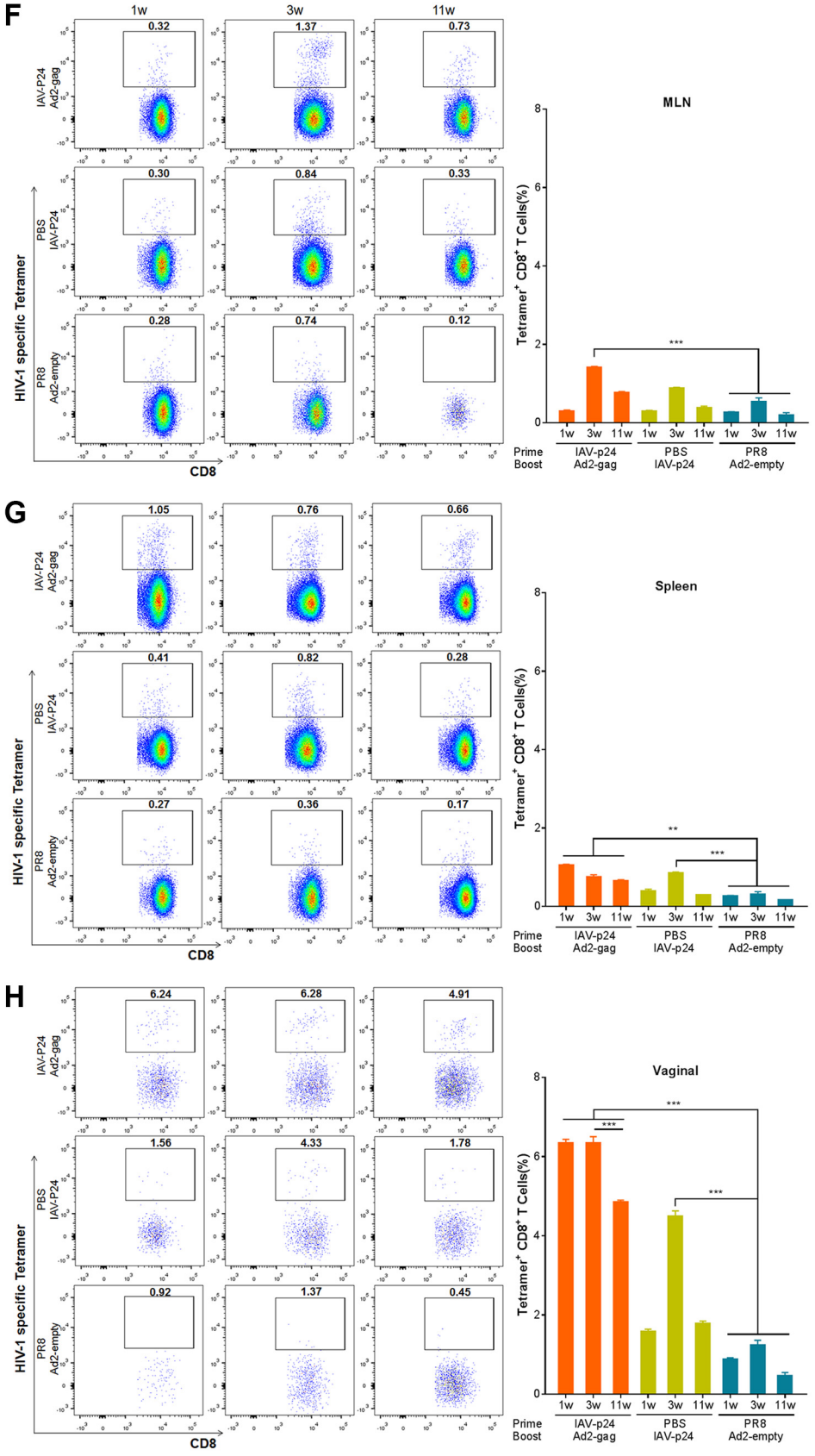

FIG 7 (Continued)

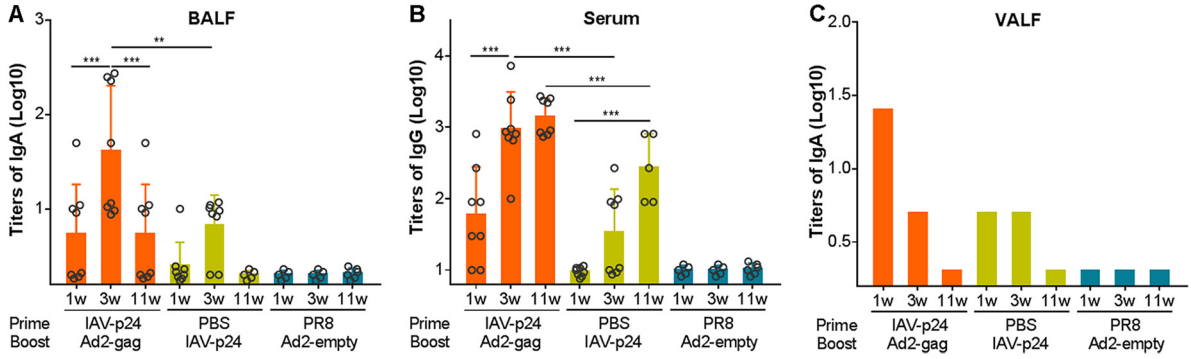

FIG 8 Dynamics of the P24-specific antibody responses elicited by the IAV-p24 prime plus Ad2-gag boost regimen. (A) P24-specific IgA antibodies in the BALF. (B) P24-specific IgG antibodies in the serum. (C) P24-specific IgA antibodies in the VALF. BALF, serum, and VALF samples were serially diluted and the P24-specific IgA and IgG antibodies were assessed by ELISA. The endpoint titers were calculated as the reciprocal of the highest dilution at which the OD_{450} values were equal to or higher than three times those of the control wells. Each circle in panels A and B represents the mean value of three technical replicates from an individual mouse. Each bar in panel C reflects the mean value of three technical replicates of the pooled VALF. Data are representative of those from two independent experiments and expressed as means ± SD ($n = 5$ to 8 per group). Comparisons among groups were conducted using one-way ANOVA. **, $P < 0.01$; ***, $P < 0.001$.

specific $CD8^+$ T cells in mice that received 1×10^4 PFU of IAV-p24, because enough lymphocytes were obtained only from these mice. Regardless of the presence of H3N2-specific antibodies, P24-specific $CD8^+$ T cells were effectively elicited in the BALF (Fig. 9E). A similar trend was observed in the spleen, although the frequencies of these cells were lower than those in the BALF (Fig. 9F). Thus, the immunogenicity of IAV-p24 is not affected by H3N2-specific antibodies, revealing a possibility to evade the anti-vector immunity by replacing the surface proteins with those derived from an antigenically distinct IAV strain.

DISCUSSION

It has been recognized that $CD8^+$ T cells and broadly neutralizing antibodies may both be critical for protection against HIV-1 infection (8, 32). Heterologous prime-boost regimens based on viral vectors are able to induce such immune responses and have been extensively developed (8, 17, 33–35). Several prime-boost regimens have shown protective efficacy in SIV-infected NHPs (9, 10). Novel viral vectors, especially those able to replicate on the mucosal surface, are desirable for the development of an efficacious HIV-1 vaccine. We show that IAV-p24 has good propagation capacity in embryonic eggs and is attenuated in mice (Fig. 1 and 2). Although a single dose of IAV-p24 elicits only moderate HIV-specific CMI responses (Fig. 3), the IAV-p24 prime plus Ad2-gag boost regimen induces robust and long-lasting CMI responses. Importantly, significant P24-specific $CD8^+$ T-cell and antibody responses are generated in both airway and vaginal mucosae (Fig. 4 and 8). These merits make IAV-p24 a promising mucosa-targeted priming vaccine against HIV-1.

One advantage of an IAV vector is that its surface proteins can be conveniently replaced with those derived from an antigenically distinct strain (28). This is important for the application of IAV-vectored vaccines in humans. The circulation of seasonal IAVs usually leads to a high seroprevalence of anti-IAV antibodies in regions of endemicity (36), which may impair the immunogenicity of an IAV vector based on these particular strains, either as a priming or as a booster vaccine. Since there are 18 known HA subtypes and 11 known NA subtypes (37), IAV vectors can be engineered with heterosubtypic surface proteins and thus bypass the preexisting anti-vector antibodies. Indeed, H3N2-specific antibodies do not reduce the immunogenicity of IAV-p24, which is based on the PR8 strain (Fig. 9). Naturally, IAV surface proteins are undergoing constant mutation, which results in multiple variants in each HA and NA subtype. According to the "original antigenic sin" concept, the preexisting antibodies may be focused on particular epitopes

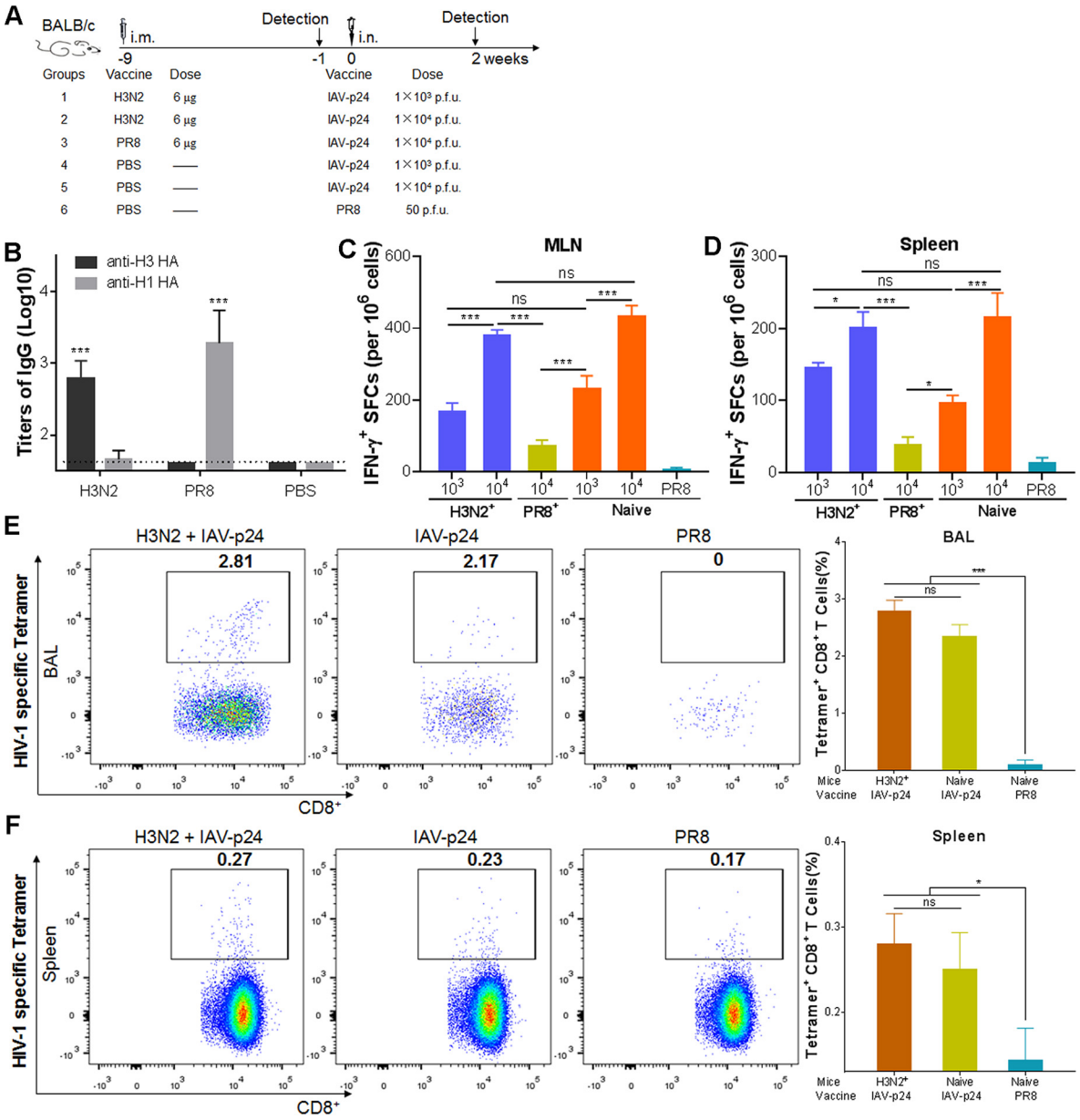

FIG 9 Immunogenicity of IAV-p24 in the presence or absence of preexisting immunity against H3N2 or PR8. (A) Schematic diagram of the experiment design. Six-week-old BALB/c mice were i.m. preimmunized with inactivated H3N2 or PR8 at 9 weeks before IAV-p24 immunization. At 1 week before IAV-p24 immunization, IgG antibodies against H1 HA (PR8 strain) or H3 HA (A/Victoria/361/2011 strain) in the serum samples were tested. At 2 weeks after IAV-p24 immunization, mice were sacrificed and lymphocytes were isolated. (B) IgG antibodies against H1 HA and H3 HA in the serum. The endpoint titers were calculated as the reciprocal of the highest dilution at which the OD_{450} values were equal to or higher than three times those of the control wells. For the H3N2 preimmunization group, $n = 10$; for the PR8 preimmunization group, $n = 5$; for the PBS group, $n = 15$. (C) IFN-γ-secreting cells in the MLN. (D) IFN-γ-secreting cells in the spleen. Lymphocytes from each group of mice ($n = 5$) were examined by ELISpot assay. (E) P24-specific $CD8^+$ T cells in total $CD8^+$ T cells from the BALF. (F) P24-specific $CD8^+$ T cells in total $CD8^+$ T cells from the spleen. P24-specific $CD8^+$ T cells were assessed by MHC-tetramer staining. In each panel, representative flow cytometry dot plot graphs (left) and the frequencies of $tetramer^+$ $CD8^+$ T cells (right) are shown. Data are representative of those from two independent experiments and expressed as means ± SD. Comparisons among groups were conducted using one-way ANOVA. *, $P < 0.05$; ***, $P < 0.001$.

during early life exposure. These antibodies may be inadequate to block the infection with a subsequent IAV that contains mutations in these epitopes (38). In this regard, there are theoretically a large number of HA and NA proteins for choice. However, it is ideal to determine the subtypes to which a population has not been widely exposed yet, and the highly virulent ones should be excluded. In addition, more attenuation may be

introduced to further enhance the safety profile of the replication-competent IAV vector. Nevertheless, the IAV vector described in this report can be improved using a selected HA and NA subtype or variant (39).

Several IAV vRNA segments, including PB2, HA, NA, and NS1, tolerate the insertion of foreign sequences (22, 23, 25, 29, 30, 40, 41). We chose the NA segment to express an HIV-1 antigen because (i) the NA segment is relatively small compared to PB2 and HA segments and thus is able to carry a larger exogenous sequence, and (ii) unlike the NS segment, which encodes NS1 and NS2 via mRNA splicing, the NA segment encodes only the NA protein and is flexible to be converted into a bicistronic vRNA. It has been shown that inserting an *egfp* gene into the 3′-terminal coding region of NA vRNA has slightly more deleterious effects on the NA activity and the growth capacity of IAV than inserting the *egfp* gene into the 5′ terminus (29). We thus inserted the HIV-1 *p24* gene into the 5′-terminal coding region. The *p24* gene is well tolerated in the bicistronic NA vRNA, as evidenced by the genome stability of IAV-p24 during serial passages (Fig. 1). IAV-p24 has a decreased growth capacity in embryonic eggs but still grows to a high titer (Fig. 1). Notably, the pathogenicity of IAV-p24 in BALB/c mice is greatly attenuated (Fig. 2), indicating that the insertion of an exogenous sequence into the NA segment reduces the virulence of IAV. IAV vectors carrying other exogenous genes via a similar strategy also show a slightly reduced growth capacity in embryonic eggs and a sharply attenuated virulence in mice (30). Our IAV vector, if introduced with cold-adaptive mutations (28), may have enhanced safety for application in humans.

As a respiratory pathogen, IAV induces both systemic and mucosal immune responses (28). Vaginal immunization with an IAV vector carrying one HIV-1 epitope elicits a long-lasting HIV-specific CTL memory in the vaginal tract (42). This is of particular significance because more than 90% of HIV-1 infections occur via a mucosal route (2, 43). Because the P24 protein is largely expressed in the cytoplasm, it may be processed in the cytosol by the proteasome and presented by the major histocompatibility complex (MHC) class I. The $CD8^+$ T-cell response observed in the airway mucosa suggests that IAV-p24 is able to elicit mucosal CMI responses, similar to other IAV vectors (Fig. 3) (42). Using two prime-boost regimens, we showed that IAV-p24 as a priming vaccine may be better in mounting P24-specific $CD8^+$ T cells (Fig. 4). These cells, especially those secreting IFN-γ, may be critical for an HIV-1 vaccine because they are important for the control of acute HIV-1 infection (44). Most importantly, a subset of HIV-specific $CD8^+$ T cells produce two (IFN-γ and TNF-α) or even three (IFN-γ, TNF-α, and IL-2) cytokines (Fig. 5). These so-called polyfunctional $CD8^+$ T cells have been shown to be associated with effective prevention of HIV-1 infection and a great control of HIV-1 viremia (7, 8, 35). According to the "common mucosal immune system" concept, activated lymphocytes can seed outside the inductive mucosal sites and migrate to distal mucosal sites via interactions between chemokines and homing receptors (45–47). This may explain the presence of P24-specific $CD8^+$ T cells in the vaginal tracts of immunized mice (Fig. 7). Moreover, these cells show a long-term persistence in both airway and vaginal mucosae, further supporting the great potency of the IAV-p24 prime plus Ad2-gag boost regimen. These $CD8^+$ T cells, especially the polyfunctional ones, are likely to form a durable immune barrier in the most vulnerable site of HIV-1 entry, thereby providing benefits for the prevention of HIV-1 infection (43).

It should be noted that the IAV-p24 prime plus Ad2-gag boost regimen also elicits significant mucosal and systemic antibody responses specific for P24 (Fig. 6 and 8). Although most neutralizing antibodies against HIV-1 recognize the Env protein, antibodies targeting P24 may also confer protective effects, possibly through a plasmacytoid dendritic cell-reactive opsonophagocytic response (48–50). The mucosal antibody response against P24 may thus contribute to blocking HIV-1 infection in susceptible

mucosa (12, 33). An IAV vector carrying a conserved epitope derived from HIV-1 gp41 induces a neutralizing antibody response in both mucosal surface and the serum (51, 52). In that vector, the gp41 epitope is inserted into antigenic site B of the HA protein (nt positions 545 to 546). However, limited foreign fragments (one epitope to ~140 amino acids) can be incorporated in this site or in other sites of HA without deleterious effects on IAV replication (39). Our IAV vector can accommodate foreign sequences up to 800 nt in length, which enables the incorporation of more neutralizing epitopes. Thus, our IAV vector may be potentially altered to express a large fragment derived from gp41 or gp120 to provoke a neutralizing antibody response against HIV-1.

In summary, we demonstrate that IAV-p24 as a live-attenuated vaccine is able to prime robust and long-lasting HIV-specific CMI and antibody responses both systemically and in the airway and vaginal mucosae. Our results provide insights for developing a prophylactic vaccine against HIV-1 infection.

MATERIALS AND METHODS

Cell lines. HEK293 (CRL-1573) and MDCK (CCL-34) cells were purchased from the American Type Culture Collection (ATCC) and cultured in Dulbecco's modified Eagle medium (DMEM; Thermo Fisher Scientific) containing 1% penicillin-streptomycin (PS) and 10% fetal bovine serum (FBS; Thermo Fisher Scientific).

Viruses. IAV-p24 was constructed as previously described (29, 30). In brief, the coding sequence for the *p24* gene of an HIV-1_01_AE isolate (GenBank accession no. JX960604.1) was codon optimized, synthesized, and inserted into the pM-PR8NA plasmid to obtain pM-PR8NA+p24. The chimeric NA vRNA contains the following elements (3′ to 5′): 3′ NCR, NA coding region, 2A sequence, *p24* gene, a stop codon, 5′ 157 nt of the NA coding region, and 5′ NCR. IAV-p24 was rescued by transfecting pM-PR8NA+p24 and the other seven genomic plasmids into HEK293-MDCK cell cocultures. One day later, cells were added with 1 μg/ml of tosylsulfonyl phenylalanyl chloromethyl ketone (TPCK)-treated trypsin (Merck). Culture media were then harvested and injected into the allantoic cavities of 9-day-old embryonic chicken eggs. Finally, allantoic fluids were harvested and IAV-p24 was purified by sucrose density gradient centrifugation. Wild-type PR8 and H3N2 viruses were propagated and purified similarly. Purified viruses were stored in PBS containing 0.5% bovine serum albumin (BSA; Sigma-Aldrich) at –80°C.

Replication-incompetent Ad2-gag was constructed as previously described (53, 54). In brief, the coding sequence for the *gag* gene of the same HIV-1_01_AE isolate was codon optimized, synthesized and inserted into pGA1 to obtain pGA1-gag. pGA1-gag was linearized and subjected to homologous recombination with linearized pAd2-empty (of which the E1 and E3 genes were deleted) in *Escherichia coli* BJ5183 competent cells. The resultant pAd2-gag and pAd2-empty were linearized and transfected into HEK293 cells to rescue Ad2-gag and Ad2-empty, respectively. Finally, Ad2-gag and Ad2-empty were propagated in HEK293 cells, purified by cesium chloride density gradient centrifugation, and stored at –80°C.

Animals. Six to eight-week-old female BALB/c mice were purchased from Beijing Vital River Laboratory Animal Technology Co. Ltd. and housed in the Animal Experimental Center of Guangzhou Institutes of Biomedicine and Health (GIBH), according to the guidelines set by the Association for the Assessment and Accreditation of Laboratory Animal Care. The experimental protocols were approved by the Institutional Animal Care and Use Committee of GIBH.

Plaque-forming assay. MDCK cells (~100% confluent) were infected with serially diluted IAV-p24 or PR8 stocks for 2 h and then overlaid with 1× minimal essential medium (MEM) containing 0.6% agarose, 0.4% BSA, and 1 μg/ml of TPCK-treated trypsin. Three days later, cells were fixed with 4% paraformaldehyde, permeabilized with 0.5% Triton X-100, and labeled with anti-PR8 mouse serum. Plaques were labeled with horseradish peroxidase (HRP)-conjugated goat anti-mouse IgG (Proteintech) and developed with an AEC (3-amino-9-ethylcarbozole) kit (Merck).

Western blot analysis. In brief, MDCK cells were infected with IAV-p24 or PR8 at 0.5 PFU per cell. At 24 h after infection, cell lysates were harvested and subjected to SDS-PAGE. After transfer, membranes were incubated with monoclonal antibodies against P24 (Abcam) or H1N1 NP (SouthernBiotech). Finally, membranes were incubated with HRP-conjugated secondary antibodies and developed by chemiluminescent HRP substrate (Merck).

Growth curve and serial-passaging assay. In brief, 9-day-old embryonic eggs were injected with 50 PFU of IAV-p24 or PR8. At 12, 24, 36, and 48 h after infection, allantoic fluids were harvested and live virions were titrated by plaque-forming assay. For the serial-passaging assay, 9-day-old embryonic eggs were injected with 50 PFU of IAV-p24. At 2 days after injection, allantoic fluids were harvested. Live virions were titrated and subjected to the next passage. A total of 9 passages were performed.

Immunofluorescence assay. In brief, 80% confluent MDCK cells were infected with IAV-p24 or PR8 at 0.1 PFU per cell. At 36 h after infection, cells were fixed, permeabilized, and labeled with a rabbit anti-HA polyclonal antibody (Thermo Fisher Scientific) and a mouse anti-P24 monoclonal antibody (clone 39/5.4A; Abcam). Subsequently, cells were incubated with fluorescein isothiocyanate (FITC)-conjugated goat anti-rabbit IgG (Thermo Fisher Scientific) and phycoerythrin

(PE)-conjugated goat anti-mouse IgG (Beyotime). Finally, cells were stained with 4′,6-diamino-2-phenylindole (DAPI; Beyotime) and imaged under a fluorescence microscope (Eclipse Ti-U; Nikon).

RT-PCR. Total RNAs were extracted from the allantoic fluids using TRIzol reagent (Thermo Fisher Scientific). cDNAs were prepared by reverse transcription-PCR (RT-PCR), and the chimeric NA vRNA and *p24* gene were amplified by PCR using the following primer pairs: for chimeric NA vRNA (5′ to 3′), forward, CCAGCAAAAGCAGGGGT, and reverse, AGCACCGTCTGGCCAAG, and for the *p24* gene (5′ to 3′), forward, GCATGATTGTGCAGAATGCCCAG, and reverse, GTTTACTTGTGGGATGGGCCG. The PCR products were subjected to electrophoresis using 1% agarose gels.

Viral pathogenicity in mice. In brief, 8-week-old female BALB/c mice ($n = 10$ per group) were anesthetized by isoflurane inhalation and i.n. infected with IAV-p24 at 10-fold-increasing doses from 1×10^3 to 1×10^5 PFU per mouse in 50 μl of PBS. Mice that received 1×10^3 PFU of PR8 or 50 μl of PBS were used as controls. The body weight was monitored daily. Mice that lost more than 25% of initial body weight or showed severe symptoms were scored as dead and euthanized. Five mice from each group were sacrificed on day 5 after infection. Fresh lung tissues were homogenized and the supernatants were subjected to plaque-forming assay.

Immunization. To assess the immunogenicity of IAV-p24, 8-week-old female BALB/c mice ($n = 5$ per group) were i.n. immunized with 1×10^4 PFU of IAV-p24 or with 50 PFU of PR8. Two weeks later, mice were sacrificed. Sera, BALF, MLN, and spleen were harvested.

To assess the immune responses elicited by the prime-boost regimens, 8-week-old female BALB/c mice ($n = 5$ per group) were i.n. immunized with 1×10^4 PFU of IAV-p24 or with 1×10^7 v.p. of Ad2-gag. Three weeks later, mice were i.n. boosted with 1×10^7 v.p. of Ad2-gag or with 1×10^4 PFU of IAV-p24, respectively. Control mice were i.n. immunized with one dose of either 1×10^4 PFU of IAV-p24 or 1×10^7 v.p. of Ad2-gag or two doses of either 50 PFU of PR8 or 1×10^7 v.p. of Ad2-empty. Two weeks after the final immunization, mice were sacrificed and sampled as described above.

To assess the dynamics of immunization-induced HIV-specific immune responses, 8-week-old female BALB/c mice ($n = 24$ per group) were i.n. primed with 1×10^4 PFU of IAV-p24, followed by an i.n. boost with 1×10^7 v.p. of Ad2-gag at 3 weeks after priming. Control mice were i.n. immunized with one dose of 1×10^4 PFU of IAV-p24 or with one dose of 50 PFU of PR8 followed by one dose of 1×10^7 v.p. of Ad2-empty. At 1, 3, and 11 weeks after the final immunization, mice were sacrificed and the sera, BALF, MLN, spleen, VALF, and vaginal tract tissues were harvested.

To assess the impacts of preexisting antibodies on the immunogenicity of IAV-p24, 6-week-old female BALB/c mice were i.m. immunized with H3N2 ($n = 10$) or PR8 ($n = 5$) viruses (equivalent to $\sim$6 μg of HA protein per mouse) that were inactivated by 0.2% β-propiolactone and added with alum adjuvant (Thermo Fisher Scientific), or they were i.n. inoculated with PBS ($n = 15$). Eight weeks later, serum samples were collected and subjected to ELISA. Mice were then i.n. immunized with 1×10^3 or 1×10^4 PFU of IAV-p24 or with 50 PFU of PR8. At 2 weeks after immunization, mice were sacrificed and the BALF, MLN, and spleens were harvested.

Lymphocyte isolation. MLN and spleens were dissociated into single-cell suspensions (Dakewe Biotech) and passed through a 200-gauge stainless mesh. Single-cell suspensions were centrifuged at 800 $\times$ *g* at 25°C for 30 min, and lymphocytes were collected from the interphase. BALFs were centrifuged at 400 $\times$ *g* at 4°C for 10 min. Vaginal tract tissues were digested with collagenase type VIII (450 to 500 U/ml) and 1.25 mg/ml of DNase I (Merck). Digested cells were collected and purified with a 40%/70% Percoll gradient (Merck). All cells were washed and resuspended in R10 (RPMI 1640 containing 10% FBS, 1% PS, 2 mM L-glutamine, 5.5 mM 2-mercaptoethanol, 10 mM HEPES, and 1 mM sodium pyruvate).

IFN-γ ELISpot assay. The ELISpot assay was performed as previously described (53). In brief, lymphocytes were seeded into ELISpot plates that were precoated with an IFN-γ-specific capture antibody (U-CyTech biosciences) and then stimulated with synthetized peptide pools corresponding to HIV-1_01_AE Gag (2 μg/ml of each peptide; Chinese Peptide) or concanavalin A (ConA; 10 ng/ml) at 37°C for 24 h. Unstimulated cells were used as controls. The plates were then incubated with the detection antibody and alkaline phosphatase-labeled streptavidin (Thermo Fisher Scientific). Finally, spots were developed with 1-Step nitroblue tetrazolium/5-bromo-4-chloro-3-indolylphosphate (NBT/BCIP) substrate solution (Thermo Fisher Scientific) and counted by ImmunoSpot 7.0.11.0.

MHC-tetramer staining. Lymphocytes were first stained with a viability dye (LIVE/DEAD fixable aqua dead cell stain; Thermo Fisher Scientific) at 4°C for 20 min. The Fc receptors were then blocked with a CD16/32 antibody (TruStain fcX; BioLegend) for 10 min. Subsequently, cells were labeled with PE-conjugated H-2K^d HIV-1 gag tetramer (AMQMLKETI; HelixGen) and the following surface antibodies: CD3-Pacific Blue, CD4-allophycocyanin (APC), and CD8-FITC (BD Biosciences). Finally, cells were analyzed by flow cytometry (LSRFortessa; BD Biosciences).

Intracellular cytokine staining. Lymphocytes were added to 96-well plates and stimulated with Gag peptide pools (2 μg/ml of each peptide) or with 40 ng/ml of phorbol 12-myristate-13-acetate and 1,000 ng/ml of ionomycin (*P*+*I*; Merck). Unstimulated cells were used as controls. After 2 h of incubation, brefeldin A (10 μg/ml; BD Biosciences) was added. After an additional 10 h of incubation, cells were harvested and stained with a viability dye at 4°C for 20 min, followed by a 10-min Fc blocking and a 30-min staining with surface antibodies (CD3-Pacific Blue, CD4-APC, and CD8-FITC). Cells were then permeabilized, stained with intracellular antibodies (IFN-γ-Alexa-700 [BioLegend] and IL-2-PE and TNF-α-APC-CY7 [BD Biosciences]), and analyzed by flow cytometry.

ELISA. In brief, 96-well ELISA plates were coated with HIV-1 P24 protein (Abcam) at 50 ng/well. Serum, BALF, or VALF samples were serially diluted and added to the plates. P24-specific IgG and IgA antibodies were examined using an HRP-conjugated goat anti-mouse IgG or IgA antibody (Bio-Rad). The plates were developed with tetramethylbenzidine (TMB) substrate, stopped with 1 mM sulfuric acid, and read at 450 nm using a microplate reader. To assess the IAV-specific antibodies, plates were coated with PR8 HA protein or H3N2 HA protein (11684-V08H and 40145-V08B, respectively; SinoBiological) at 50 ng/well. HA-specific IgG antibodies in the sera were tested similarly. Endpoint titers were calculated as the reciprocal of the highest dilutions at which the values for optical density at 450 nm (OD_{450}) were equal to or higher than three times the control wells.

Data analysis. Flow cytometry data were analyzed using FlowJo, version 10 (Tree Star, Inc.). Illustrations were generated using Microsoft PowerPoint, version 2010 (Microsoft). Data graphs were generated using GraphPad Prism, version 7 (GraphPad Software). Figures were created using Adobe Photoshop, version CS2 (Adobe Inc.). Comparison of the survival rates was performed using the log rank test. Comparison between two groups was conducted using unpaired two-tailed Student's *t* test. Other statistical analyses were performed using one-way analysis of variance (ANOVA). *P* values less than 0.05 were considered statistically significant.

ACKNOWLEDGMENTS

We thank Cuie Li and Zhi Wang for their technical assistance.

This study was supported by the National Natural Science Foundation of China (31470892, 82061138006, and 81670536), the Strategic Priority Research Program of the Chinese Academy of Sciences (XDB29050701), the National Science and Technology Major Project (2017ZX10204401003, 2018ZX10101003005, and 2018ZX10301404-003-002), and the Guangzhou Health Care and Cooperative Innovation Major Project (201803040004).

L.H. is an employee of Guangzhou nBiomed, Ltd. The other authors declare no competing financial interests.

REFERENCES

1. World Health Organization. 2020. Latest HIV estimates and updates on HIV policies uptake, November 2020. https://www.who.int/health-topics/hiv-aids#tab=tab_1.
2. Haase AT. 2011. Early events in sexual transmission of HIV and SIV and opportunities for interventions. Annu Rev Med 62:127–139. https://doi.org/10.1146/annurev-med-080709-124959.
3. Richman DD, Margolis DM, Delaney M, Greene WC, Hazuda D, Pomerantz RJ. 2009. The challenge of finding a cure for HIV infection. Science 323:1304–1307. https://doi.org/10.1126/science.1165706.
4. Cuevas JM, Geller R, Garijo R, Lopez-Aldeguer J, Sanjuan R. 2015. Extremely high mutation rate of HIV-1 in vivo. PLoS Biol 13:e1002251. https://doi.org/10.1371/journal.pbio.1002251.
5. Janes H, Friedrich DP, Krambrink A, Smith RJ, Kallas EG, Horton H, Casimiro DR, Carrington M, Geraghty DE, Gilbert PB, McElrath MJ, Frahm N. 2013. Vaccine-induced gag-specific T cells are associated with reduced viremia after HIV-1 infection. J Infect Dis 208:1231–1239. https://doi.org/10.1093/infdis/jit322.
6. Janes HE, Cohen KW, Frahm N, De Rosa SC, Sanchez B, Hural J, Magaret CA, Karuna S, Bentley C, Gottardo R, Finak G, Grove D, Shen M, Graham BS, Koup RA, Mulligan MJ, Koblin B, Buchbinder SP, Keefer MC, Adams E, Anude C, Corey L, Sobieszczyk M, Hammer SM, Gilbert PB, McElrath MJ. 2017. Higher T-cell responses induced by DNA/rAd5 HIV-1 preventive vaccine are associated with lower HIV-1 infection risk in an efficacy trial. J Infect Dis 215:1376–1385. https://doi.org/10.1093/infdis/jix086.
7. Betts MR, Nason MC, West SM, De Rosa SC, Migueles SA, Abraham J, Lederman MM, Benito JM, Goepfert PA, Connors M, Roederer M, Koup RA. 2006. HIV nonprogressors preferentially maintain highly functional HIV-specific CD8+ T cells. Blood 107:4781–4789. https://doi.org/10.1182/blood-2005-12-4818.
8. Korber B, Fischer W. 2020. T cell-based strategies for HIV-1 vaccines. Hum Vaccin Immunother 16:713–722. https://doi.org/10.1080/21645515.2019.1666957.
9. Sun C, Chen Z, Tang X, Zhang Y, Feng L, Du Y, Xiao L, Liu L, Zhu W, Chen L, Zhang L. 2013. Mucosal priming with a replicating-vaccinia virus-based vaccine elicits protective immunity to simian immunodeficiency virus challenge in rhesus monkeys. J Virol 87:5669–5677. https://doi.org/10.1128/JVI.03247-12.
10. Hansen SG, Ford JC, Lewis MS, Ventura AB, Hughes CM, Coyne-Johnson L, Whizin N, Oswald K, Shoemaker R, Swanson T, Legasse AW, Chiuchiolo MJ, Parks CL, Axthelm MK, Nelson JA, Jarvis MA, Piatak M, Jr, Lifson JD, Picker LJ. 2011. Profound early control of highly pathogenic SIV by an effector memory T-cell vaccine. Nature 473:523–527. https://doi.org/10.1038/nature10003.
11. Hansen SG, Sacha JB, Hughes CM, Ford JC, Burwitz BJ, Scholz I, Gilbride RM, Lewis MS, Gilliam AN, Ventura AB, Malouli D, Xu G, Richards R, Whizin N, Reed JS, Hammond KB, Fischer M, Turner JM, Legasse AW, Axthelm MK, Edlefsen PT, Nelson JA, Lifson JD, Fruh K, Picker LJ. 2013. Cytomegalovirus vectors violate CD8+ T cell epitope recognition paradigms. Science 340:1237874. https://doi.org/10.1126/science.1237874.
12. Burton DR, Hangartner L. 2016. Broadly neutralizing antibodies to HIV and their role in vaccine design. Annu Rev Immunol 34:635–659. https://doi.org/10.1146/annurev-immunol-041015-055515.
13. Xu L, Pegu A, Rao E, Doria-Rose N, Beninga J, McKee K, Lord DM, Wei RR, Deng G, Louder M, Schmidt SD, Mankoff Z, Wu L, Asokan M, Beil C, Lange C, Leuschner WD, Kruip J, Sendak R, Kwon YD, Zhou T, Chen X, Bailer RT, Wang K, Choe M, Tartaglia LJ, Barouch DH, O'Dell S, Todd JP, Burton DR, Roederer M, Connors M, Koup RA, Kwong PD, Yang ZY, Mascola JR, Nabel GJ. 2017. Trispecific broadly neutralizing HIV antibodies mediate potent SHIV protection in macaques. Science 358:85–90. https://doi.org/10.1126/science.aan8630.
14. Haynes BF, Gilbert PB, McElrath MJ, Zolla-Pazner S, Tomaras GD, Alam SM, Evans DT, Montefiori DC, Karnasuta C, Sutthent R, Liao HX, DeVico AL, Lewis GK, Williams C, Pinter A, Fong Y, Janes H, DeCamp A, Huang Y, Rao M, Billings E, Karasavvas N, Robb ML, Ngauy V, de Souza MS, Paris R, Ferrari G, Bailer RT, Soderberg KA, Andrews C, Berman PW, Frahm N, De Rosa SC, Alpert MD, Yates NL, Shen X, Koup RA, Pitisuttithum P, Kaewkungwal J, Nitayaphan S, Rerks-Ngarm S, Michael NL, Kim JH. 2012. Immune-correlates analysis of an HIV-1 vaccine efficacy trial. N Engl J Med 366:1275–1286. https://doi.org/10.1056/NEJMoa1113425.
15. Barouch DH. 2010. Novel adenovirus vector-based vaccines for HIV-1. Curr Opin HIV AIDS 5:386–390. https://doi.org/10.1097/COH.0b013e32833cfe4c.
16. Sekaly RP. 2008. The failed HIV Merck vaccine study: a step back or a launching point for future vaccine development? J Exp Med 205:7–12. https://doi.org/10.1084/jem.20072681.
17. Brown SA, Surman SL, Sealy R, Jones BG, Slobod KS, Branum K, Lockey TD, Howlett N, Freiden P, Flynn P, Hurwitz JL. 2010. Heterologous prime-

boost HIV-1 vaccination regimens in pre-clinical and clinical trials. Viruses 2:435–467. https://doi.org/10.3390/v2020435.
18. Parks CL, Picker LJ, King CR. 2013. Development of replication-competent viral vectors for HIV vaccine delivery. Curr Opin HIV AIDS 8:402–411. https://doi.org/10.1097/COH.0b013e328363d389.
19. Hoffmann E, Neumann G, Kawaoka Y, Hobom G, Webster RG. 2000. A DNA transfection system for generation of influenza A virus from eight plasmids. Proc Natl Acad Sci U S A 97:6108–6113. https://doi.org/10.1073/pnas.100133697.
20. Zhang S, Sun F, Ren T, Duan Y, Gu H, Lai C, Wang Z, Zhang P, Wang X, Yang P. 2017. Immunogenicity of an influenza virus-vectored vaccine carrying the hepatitis C virus protein epitopes in mice. Antiviral Res 145:168–174. https://doi.org/10.1016/j.antiviral.2017.07.015.
21. Zhang P, Gu H, Bian C, Liu N, Li Z, Duan Y, Zhang S, Wang X, Yang P. 2014. Characterization of recombinant influenza A virus as a vector expressing respiratory syncytial virus fusion protein epitopes. J Gen Virol 95:1886–1891. https://doi.org/10.1099/vir.0.064105-0.
22. de Goede AL, Boers PH, Dekker LJ, Osterhaus AD, Gruters RA, Rimmelzwaan GF. 2009. Characterization of recombinant influenza A virus as a vector for HIV-1 p17Gag. Vaccine 27:5735–5739. https://doi.org/10.1016/j.vaccine.2009.07.032.
23. Sexton A, De Rose R, Reece JC, Alcantara S, Loh L, Moffat JM, Laurie K, Hurt A, Doherty PC, Turner SJ, Kent SJ, Stambas J. 2009. Evaluation of recombinant influenza virus-simian immunodeficiency virus vaccines in macaques. J Virol 83:7619–7628. https://doi.org/10.1128/JVI.00470-09.
24. Reece JC, Alcantara S, Gooneratne S, Jegaskanda S, Amaresena T, Fernandez CS, Laurie K, Hurt A, O'Connor SL, Harris M, Petravic J, Martyushev A, Grimm A, Davenport MP, Stambas J, De Rose R, Kent SJ. 2013. Trivalent live attenuated influenza-simian immunodeficiency virus vaccines: efficacy and evolution of cytotoxic T lymphocyte escape in macaques. J Virol 87:4146–4160. https://doi.org/10.1128/JVI.02645-12.
25. Ferko B, Stasakova J, Sereinig S, Romanova J, Katinger D, Niebler B, Katinger H, Egorov A. 2001. Hyperattenuated recombinant influenza A virus nonstructural-protein-encoding vectors induce human immunodeficiency virus type 1 Nef-specific systemic and mucosal immune responses in mice. J Virol 75:8899–8908. https://doi.org/10.1128/JVI.75.19.8899-8908.2001.
26. Krammer F. 2020. SARS-CoV-2 vaccines in development. Nature 586:516–527. https://doi.org/10.1038/s41586-020-2798-3.
27. Padilla-Quirarte HO, Lopez-Guerrero DV, Gutierrez-Xicotencatl L, Esquivel-Guadarrama F. 2019. Protective antibodies against influenza proteins. Front Immunol 10:1677. https://doi.org/10.3389/fimmu.2019.01677.
28. Li J, Arevalo MT, Zeng M. 2013. Engineering influenza viral vectors. Bioengineered 4:9–14. https://doi.org/10.4161/bioe.21950.
29. Li F, Feng L, Pan W, Dong Z, Li C, Sun C, Chen L. 2010. Generation of replication-competent recombinant influenza A viruses carrying a reporter gene harbored in the neuraminidase segment. J Virol 84:12075–12081. https://doi.org/10.1128/JVI.00046-10.
30. Pan W, Dong Z, Li F, Meng W, Feng L, Niu X, Li C, Luo Q, Li Z, Sun C, Chen L. 2013. Visualizing influenza virus infection in living mice. Nat Commun 4:2369. https://doi.org/10.1038/ncomms3369.
31. Chakraborty S, Rahman T, Chakravorty R. 2014. Characterization of the protective HIV-1 CTL epitopes and the corresponding HLA class I alleles: a step towards designing CTL based HIV-1 vaccine. Adv Virol 2014:321974. https://doi.org/10.1155/2014/321974.
32. Corey L, Gilbert PB, Tomaras GD, Haynes BF, Pantaleo G, Fauci AS. 2015. Immune correlates of vaccine protection against HIV-1 acquisition. Sci Transl Med 7:310rv7. https://doi.org/10.1126/scitranslmed.aac7732.
33. Xu K, Acharya P, Kong R, Cheng C, Chuang GY, Liu K, Louder MK, O'Dell S, Rawi R, Sastry M, Shen CH, Zhang B, Zhou T, Asokan M, Bailer RT, Chambers M, Chen X, Choi CW, Dandey VP, Doria-Rose NA, Druz A, Eng ET, Farney SK, Foulds KE, Geng H, Georgiev IS, Gorman J, Hill KR, Jafari AJ, Kwon YD, Lai YT, Lemmin T, McKee K, Ohr TY, Ou L, Peng D, Rowshan AP, Sheng Z, Todd JP, Tsybovsky Y, Viox EG, Wang Y, Wei H, Yang Y, Zhou AF, Chen R, Yang L, Scorpio DG, McDermott AB, Shapiro L, et alet al. 2018. Epitope-based vaccine design yields fusion peptide-directed antibodies that neutralize diverse strains of HIV-1. Nat Med 24:857–867. https://doi.org/10.1038/s41591-018-0042-6.
34. Barouch DH, Tomaka FL, Wegmann F, Stieh DJ, Alter G, Robb ML, Michael NL, Peter L, Nkolola JP, Borducchi EN, Chandrashekar A, Jetton D, Stephenson KE, Li W, Korber B, Tomaras GD, Montefiori DC, Gray G, Frahm N, McElrath MJ, Baden L, Johnson J, Hutter J, Swann E, Karita E, Kibuuka H, Mpendo J, Garrett N, Mngadi K, Chinyenze K, Priddy F, Lazarus E, Laher F, Nitayapan S, Pitisuttithum P, Bart S, Campbell T, Feldman R, Lucksinger G, Borremans C, Callewaert K, Roten R, Sadoff J, Scheppler L, Weijtens M, Feddes-de Boer K, van Manen D, Vreugdenhil J, Zahn R, Lavreys L, et alet al. 2018. Evaluation of a mosaic HIV-1 vaccine in a multicentre, randomised, double-blind, placebo-controlled, phase 1/2a clinical trial (APPROACH) and in rhesus monkeys (NHP 13-19). Lancet 392:232–243. https://doi.org/10.1016/S0140-6736(18)31364-3.
35. Alayo QA, Provine NM, Penaloza-MacMaster P. 2017. Novel concepts for HIV vaccine vector design. mSphere 2:e00415-17. https://doi.org/10.1128/mSphere.00415-17.
36. Bodewes R, de Mutsert G, van der Klis FR, Ventresca M, Wilks S, Smith DJ, Koopmans M, Fouchier RA, Osterhaus AD, Rimmelzwaan GF. 2011. Prevalence of antibodies against seasonal influenza A and B viruses in children in Netherlands. Clin Vaccine Immunol 18:469–476. https://doi.org/10.1128/CVI.00396-10.
37. Tong S, Zhu X, Li Y, Shi M, Zhang J, Bourgeois M, Yang H, Chen X, Recuenco S, Gomez J, Chen LM, Johnson A, Tao Y, Dreyfus C, Yu W, McBride R, Carney PJ, Gilbert AT, Chang J, Guo Z, Davis CT, Paulson JC, Stevens J, Rupprecht CE, Holmes EC, Wilson IA, Donis RO. 2013. New World bats harbor diverse influenza A viruses. PLoS Pathog 9:e1003657. https://doi.org/10.1371/journal.ppat.1003657.
38. Vatti A, Monsalve DM, Pacheco Y, Chang C, Anaya JM, Gershwin ME. 2017. Original antigenic sin: a comprehensive review. J Autoimmun 83:12–21. https://doi.org/10.1016/j.jaut.2017.04.008.
39. Gerlach T, Elbahesh H, Saletti G, Rimmelzwaan GF. 2019. Recombinant influenza A viruses as vaccine vectors. Expert Rev Vaccines 18:379–392. https://doi.org/10.1080/14760584.2019.1582338.
40. Heaton NS, Leyva-Grado VH, Tan GS, Eggink D, Hai R, Palese P. 2013. In vivo bioluminescent imaging of influenza A virus infection and characterization of novel cross-protective monoclonal antibodies. J Virol 87:8272–8281. https://doi.org/10.1128/JVI.00969-13.
41. Reuther P, Gopfert K, Dudek AH, Heiner M, Herold S, Schwemmle M. 2015. Generation of a variety of stable influenza A reporter viruses by genetic engineering of the NS gene segment. Sci Rep 5:11346. https://doi.org/10.1038/srep11346.
42. Garulli B, Kawaoka Y, Castrucci MR. 2004. Mucosal and systemic immune responses to a human immunodeficiency virus type 1 epitope induced upon vaginal infection with a recombinant influenza A virus. J Virol 78:1020–1025. https://doi.org/10.1128/jvi.78.2.1020-1025.2004.
43. Demberg T, Robert-Guroff M. 2009. Mucosal immunity and protection against HIV/SIV infection: strategies and challenges for vaccine design. Int Rev Immunol 28:20–48. https://doi.org/10.1080/08830180802684331.
44. Ndhlovu ZM, Kamya P, Mewalal N, Kloverpris HN, Nkosi T, Pretorius K, Laher F, Ogunshola F, Chopera D, Shekhar K, Ghebremichael M, Ismail N, Moodley A, Malik A, Leslie A, Goulder PJ, Buus S, Chakraborty A, Dong K, Ndung'u T, Walker BD. 2015. Magnitude and kinetics of CD8+ T cell activation during hyperacute HIV infection impact viral set point. Immunity 43:591–604. https://doi.org/10.1016/j.immuni.2015.08.012.
45. Naz RK. 2012. Female genital tract immunity: distinct immunological challenges for vaccine development. J Reprod Immunol 93:1–8. https://doi.org/10.1016/j.jri.2011.09.005.
46. Czerkinsky C, Prince SJ, Michalek SM, Jackson S, Russell MW, Moldoveanu Z, McGhee JR, Mestecky J. 1987. IgA antibody-producing cells in peripheral blood after antigen ingestion: evidence for a common mucosal immune system in humans. Proc Natl Acad Sci U S A 84:2449–2453. https://doi.org/10.1073/pnas.84.8.2449.
47. Wilson HL, Obradovic MR. 2015. Evidence for a common mucosal immune system in the pig. Mol Immunol 66:22–34. https://doi.org/10.1016/j.molimm.2014.09.004.
48. Tjiam MC, Taylor JP, Morshidi MA, Sariputra L, Burrows S, Martin JN, Deeks SG, Tan DB, Lee S, Fernandez S, French MA. 2015. Viremic HIV controllers exhibit high plasmacytoid dendritic cell-reactive opsonophagocytic IgG antibody responses against HIV-1 p24 associated with greater antibody isotype diversification. J Immunol 194:5320–5328. https://doi.org/10.4049/jimmunol.1402918.
49. Tjiam MC, Sariputra L, Armitage JD, Taylor JPA, Kelleher AD, Tan DBA, Lee S, Fernandez S, French MA. 2016. Control of early HIV-1 infection associates with plasmacytoid dendritic cell-reactive opsonophagocytic IgG antibodies to HIV-1 p24. AIDS 30:2757–2765. https://doi.org/10.1097/QAD.0000000000001242.

50. French MA, Tanaskovic S, Law MG, Lim A, Fernandez S, Ward LD, Kelleher AD, Emery S. 2010. Vaccine-induced IgG2 anti-HIV p24 is associated with control of HIV in patients with a 'high-affinity' Fc gamma RIIa genotype. AIDS 24:1983–1990. https://doi.org/10.1097/QAD.0b013e32833c1ce0.
51. Muster T, Guinea R, Trkola A, Purtscher M, Klima A, Steindl F, Palese P, Katinger H. 1994. Cross-neutralizing activity against divergent human immunodeficiency virus type 1 isolates induced by the gp41 sequence ELDKWAS. J Virol 68:4031–4034. https://doi.org/10.1128/JVI.68.6.4031-4034.1994.
52. Muster T, Ferko B, Klima A, Purtscher M, Trkola A, Schulz P, Grassauer A, Engelhardt OG, Garcia-Sastre A, Palese P. 1995. Mucosal model of immunization against human immunodeficiency virus type 1 with a chimeric influenza virus. J Virol 69:6678–6686. https://doi.org/10.1128/JVI.69.11.6678-6686.1995.
53. Feng Y, Li C, Hu P, Wang Q, Zheng X, Zhao Y, Shi Y, Yang S, Yi C, Feng Y, Wu C, Qu L, Xu W, Li Y, Sun C, Gao FG, Xia X, Feng L, Chen L. 2018. An adenovirus serotype 2-vectored ebolavirus vaccine generates robust antibody and cell-mediated immune responses in mice and rhesus macaques. Emerg Microbes Infect 7:101. https://doi.org/10.1038/s41426-018-0102-5.
54. Liu X, Qu L, Ye X, Yi C, Zheng X, Hao M, Su W, Yao Z, Chen P, Zhang S, Feng Y, Wang Q, Yan Q, Li P, Li H, Li F, Pan W, Niu X, Xu R, Feng L, Chen L. 2018. Incorporation of NS1 and prM/M are important to confer effective protection of adenovirus-vectored Zika virus vaccine carrying E protein. NPJ Vaccines 3:29. https://doi.org/10.1038/s41541-018-0072-6.